
ACTION HALLUCINATION IN GENERATIVE VISION-LANGUAGE-ACTION MODELS

A PREPRINT

Harold Soh and **Eugene Lim**

¹Department of Computer Science, School of Computing

²Smart Systems Institute

National University of Singapore

harold@nus.edu.sg elimwj@u.nus.edu

May 13, 2026

ABSTRACT

Robot Foundation Models, such as VLAs, promise end-to-end generative robot policies with broad generalization. Yet it remains unclear whether they fundamentally resolve the core problem of action generation in embodied settings, or overcome the long-standing challenges of robotics. We address this question by analyzing action hallucinations that violate physical constraints and their extension to plan-level failures. Focusing on latent-variable generative policies, we show that hallucinations can arise from structural mismatches between feasible robot behavior and common model architectures. We study three such barriers—topological, precision, and horizon—and show how they impose unavoidable tradeoffs. Our analysis provides mechanistic explanations for reported empirical failures of generative robot policies and suggests principled directions for improving reliability and trustworthiness, without abandoning their expressive power.

1 Introduction

Robot Foundation Models (RFMs) and Large-scale Vision-Language-Action (VLA) models (e.g., [1, 2, 3, 4]) promise a “GPT moment” for robotics: given image observations and a natural-language instruction, a single end-to-end policy produces a continuous control trajectory that solves the task. Recent generative VLAs such as $\pi_{0.5}$ [5], Gr00T N1 [4], and MolmoAct [6] combine transformer encoders with conditional flow/diffusion models that map Gaussian noise into full action trajectories. Other contenders like diffusion policies [7, 8] and flow-matching policies [9] map Gaussian noise into action chunks that are executed sequentially. These models demonstrate impressive semantic generalization, yet substantial prior work [10, 11, 12, 13, 14] has shown they also generate actions that are physically invalid, e.g., grasps through objects or plans that do not result in goal achievement. We refer to this phenomenon as *action hallucination*.

Action hallucinations matter for two reasons. First, they are safety- and reliability-critical. Unlike hallucinated text, invalid actions are executed in the physical world and can cause damage or hazardous interactions. Second, these failures may not be confined to exotic corner cases. Even a model that is highly capable *on average* can intermittently produce nonsensical actions, a risk that is amplified when robots are deployed at scale and over long periods of time.

This paper argues that part of action hallucination is *structural*: it arises from a mismatch between (i) the geometry/topology of physically valid behavior in robotics and (ii) the architectural regularities of modern generative action heads and planning pipelines. Concretely, many VLAs generate actions by sampling a *connected* latent prior (typically Gaussian noise) and decoding it through a map that is continuous in the latent (as in diffusion, flow-matching, and conditional flows). At execution time, these models are often used sequentially and/or wrapped in test-time sampling (and possible verification). This work clarifies *when* these design choices induce hallucinations (regardless of the data or model scale) and *what* changes are needed to mitigate them.

Contributions. We use largely elementary mathematical tools (topology, measure bounds, and probabilistic arguments) to construct a coherent theory of action hallucination that matches the architectural and algorithmic characteristics

arXiv:2602.06339v2 [cs.RO] 12 May 2026

of modern VLAs. This approach connects to classic insights in robotics and leads to a clean formal framework to analyze generative VLAs—the constraints of non-convexity, precision, and compounding errors are foundational to robotics [15, 16, 17] and our contribution is to study these constraints in the context of modern VLAs. Concretely, we contribute:

- A **topological impossibility result** for hallucination-free multi-mode coverage under continuous latent heads, and a quantitative **isoperimetric lower bound** connecting hallucination to decoder smoothness and mode separation.
- A **precision-barrier analysis** for contact tasks, including a lower bound and a **generative precision trilemma** (fold, collapse, or hallucinate), plus a refinement-step tradeoff that clarifies why iterative diffusion/flow-style generation helps.
- A reliability-aware analysis of **verification-guided planning** for **long-horizon tasks** that identifies when test-time compute helps and why adaptive search is needed under verifier noise.

Our theoretical analysis complements the growing body of empirical work on VLAs (e.g., [3, 6, 14, 13]) and helps clarify why VLAs work, as well as when and why they may fail. Our focus is not to develop new general mathematical theory, but rather, adapt existing tools to analyze the connection between generative models and embodied action generation. We discuss connections to recent experimental results and to practical system design choices, e.g., hybrid discrete-continuous structure, iterative refinement, and verification-guided planning.

Related Work. Hallucination has been widely studied in LLMs and VLMs, where it is typically framed as fluent generation that violates an external correctness oracle such as factuality, groundedness, or visual consistency [18, 19, 20, 21, 22]. We adopt this oracle-based view, but replace textual truthfulness with *physical and task validity* in embodied settings.

Our analysis connects three previously separate threads. First, robotics has long recognized that feasible behavior is rarely convex or safely interpolatable: obstacles induce nonconvex and disconnected free spaces [15], narrow passages make feasible connections hard to find [16, 23], and contact-rich manipulation often requires hitting thin, lower-dimensional contact sets and mode transitions [24, 25, 26, 27]. Second, prior work on deep generative models shows that continuous generators with connected latent priors cannot exactly represent disconnected target supports, leading to mode dropping or bridging samples [28, 29, 30, 31, 32, 33, 34]. In this work, we interpret these bridge samples physically; in robot action spaces, they can correspond to collisions, infeasible contacts, joint-limit violations, or actions that fall into non-progress regions. Our precision analysis likewise quantifies the density concentration needed to hit thin feasible tubes, and shows how flow/DDIM-style samplers realize this concentration through local contraction across refinement steps.

Finally, our work relates to long-horizon decision-making and verification-guided search. Multi-step planning is computationally hard [35, 36], and compounding error is a classic source of long-horizon failure in imitation learning [17]. Viewed probabilistically, long-horizon success becomes a rare event, motivating decomposition and adaptive sampling methods [37, 38]. To see if VLAs can bypass these constraints through scale or test-time compute [39, 40, 41], we formalize how horizon-induced rarity, verifier noise, and adaptive proposal mechanisms interact to reduce—or limit the reduction of—behavioral hallucinations.

2 Preliminaries

In this section, we formalize robot environments, task instances, and generative robot policies, then use this framework to define action hallucinations in embodied AI. Due to space constraints, we focus on the core ideas; full proofs, formal arguments, and additional details are deferred to the appendix.

Environment Model and Tasks. We consider a robot that operates in an environment and seeks to achieve a goal.

Definition 1 (Environment). *An environment is a tuple $\mathcal{E} = (\mathcal{S}, \mathcal{A}, \Omega, O, \mathcal{T}, \mathcal{C}_{\text{safe}})$, where $\mathcal{S} \subseteq \mathbb{R}^n$ is the true physical state space, $\mathcal{A} \subseteq \mathbb{R}^d$ is the continuous action space, Ω is the observation space, $O : \mathcal{S} \rightarrow \Omega$ is the observation map, $\mathcal{T} : \mathcal{S} \times \mathcal{A} \rightarrow \mathcal{S}$ is the transition map, and $\mathcal{C}_{\text{safe}} \subseteq \mathcal{S}$ is the set of physically consistent and constraint-satisfying states.*

Definition 2 (Goal-reaching task instance). *A task instance is $I = (\mathcal{E}, s_0, \ell, \mathcal{G}, T)$, where $s_0 \in \mathcal{C}_{\text{safe}}$ is the initial state, ℓ is the language instruction, $\mathcal{G} \subseteq \mathcal{C}_{\text{safe}}$ is the goal set, and $T \in \mathbb{N}$ is the horizon or action budget.*

An action is generic in that it may denote a target pose, joint velocity, torque command, motion primitive, or action chunk. When a is a chunk or trajectory, $\mathcal{T}(s, a)$ denotes the terminal state after execution. We use deterministic observations and dynamics for clarity; stochastic observations or transitions can be handled by replacing O and \mathcal{T} with kernels and taking the probabilities below over this additional randomness. The deterministic setting is the special case where the kernels are point masses. The set $\mathcal{C}_{\text{safe}}$ is a ground-truth physical object used to define hallucination.

VLA Contexts and Latent Action Heads. At time t , the robot observes $o_t = O(s_t)$. Let $h_t = (o_0, a_0, \dots, o_{t-1}, a_{t-1}, o_t)$ be the observation-action history. A VLA encoder maps history and language to a context $c_t = E_\phi(h_t, \ell) \in \mathcal{C}$. The context may contain image-language embeddings, proprioception, memory, or other internal representations. We define the oracle-state case as a special case $c_t = c^*(s_t, \ell)$. This setting deliberately favors the policy: the action head receives all task-relevant state information, allowing us to isolate limitations of action generation itself rather than confounding them with perceptual errors or state estimation failures. We state our main results for this oracle-state specialization, but the same arguments extend to more general settings by replacing s with the history/context.

Assumption 3 (Latent prior). *The latent space \mathcal{Z} is a nonempty, open, and path-connected subset of \mathbb{R}^m . The latent prior p_Z is absolutely continuous with respect to m -dimensional Lebesgue measure, and has a density ρ_Z such that $\rho_Z(z) > 0$ for almost every $z \in \mathcal{Z}$, and is bounded below on compact subsets of \mathcal{Z} .*

Definition 4 (Latent-head VLA policy). *A latent-head VLA policy is a map $\pi_\theta : \mathcal{C} \times \mathcal{Z} \rightarrow \mathcal{A}$. For each fixed context c , the map $z \mapsto \pi_\theta(c, z)$ is continuous. The induced action distribution is $p_\theta(\cdot | c) := (\pi_\theta(c, \cdot))_{\#} p_Z$.*

This captures continuous generative action heads such as flow matching, DDIM, and conditional flow decoders. For stochastic diffusion samplers with fresh noise injected at multiple denoising steps, one can regard the full collection of injected noise variables as the latent input. In the oracle-state case, we write $p_\theta(\cdot | s, \ell) := p_\theta(\cdot | c^*(s, \ell))$, and omit ℓ when it is fixed.

Action and Plan Hallucination. Given the structure of existing VLAs, we consider two major types of behavior hallucinations. At the low-level, an *action hallucination* is an action (or action chunk / trajectory) whose induced rollout violates physical laws or environmental constraints (e.g., teleporting the robot, penetrating a solid obstacle, or exceeding kinematic limits). At the high-level, even physically valid actions can still fail to achieve the task goal. Hence, a *plan hallucination* is a generated plan (sequence of actions) that violates constraints and/or fails to reach the goal. Plan hallucinations subsume action hallucinations but also include *goal failure*.

Definition 5 (Physical validity oracle). *For a fixed environment \mathcal{E} , define $f_{\text{phys}} : \mathcal{S} \times \mathcal{A} \rightarrow \{0, 1\}$, where $f_{\text{phys}}(s, a) = 1$ if executing a from state s respects the relevant physical and environmental constraints, and $f_{\text{phys}}(s, a) = 0$ otherwise.*

For chunks or trajectories, f_{phys} checks all intermediate states, not only the terminal state. State-dependent action/admissibility constraints, such as torque limits and task-specific feasibility constraints, are folded into f_{phys} . Define the safe action set, $A_{\text{safe}}(s) = \{a \in \mathcal{A} : f_{\text{phys}}(s, a) = 1\}$ and the forbidden/unsafe action set $A_{\text{forb}}(s) = \mathcal{A} \setminus A_{\text{safe}}(s)$.

Definition 6 (Action hallucination). *At physical state s and context c , a sampled action $a = \pi_\theta(c, z)$ is an action hallucination if $f_{\text{phys}}(s, a) = 0$. Its probability is $H_\theta(s, c) := \Pr_{Z \sim p_Z} [f_{\text{phys}}(s, \pi_\theta(c, Z)) = 0]$. In the oracle-state case, we write $H_\theta(s, \ell) := H_\theta(s, c^*(s, \ell))$, or simply $H_\theta(s)$ when ℓ is fixed.*

A closed-loop VLA induces a finite action sequence when unrolled. Given $I = (\mathcal{E}, s_0, \ell, \mathcal{G}, T)$ and i.i.d. latents $z_{0:T-1}$, define $o_t = O(s_t)$, $c_t = E_\phi(h_t, \ell)$, $a_t = \pi_\theta(c_t, z_t)$, and $s_{t+1} = \mathcal{T}(s_t, a_t)$. The induced plan is $\tau_{\theta, \phi}(I, z_{0:T-1}) := (a_0, \dots, a_{T-1}) \in \mathcal{A}^T$. Here “plan” means the grounded action sequence induced by closed-loop execution (which need not be a symbolic subtask sequence).

Definition 7 (Plan hallucination). *For an action sequence $\tau = (a_0, \dots, a_{T-1})$, let $s_{t+1} = \mathcal{T}(s_t, a_t)$ be its rollout from s_0 . Define $f_{\text{plan}}(s_0, \tau; \mathcal{G}) = 1$ iff $f_{\text{phys}}(s_t, a_t) = 1$ for all $t = 0, \dots, T-1$, and $s_T \in \mathcal{G}$. Otherwise $f_{\text{plan}}(s_0, \tau; \mathcal{G}) = 0$. A plan hallucination occurs when $f_{\text{plan}}(s_0, \tau; \mathcal{G}) = 0$ and its probability on instance I is $H_{\theta, \phi}^{\text{plan}}(I) := \Pr [f_{\text{plan}}(s_0, \tau_{\theta, \phi}(I, Z_{0:T-1}); \mathcal{G}) = 0]$.*

We call I solvable if some $\tau \in \mathcal{A}^T$ satisfies $f_{\text{plan}}(s_0, \tau; \mathcal{G}) = 1$, and focus on solvable instances.

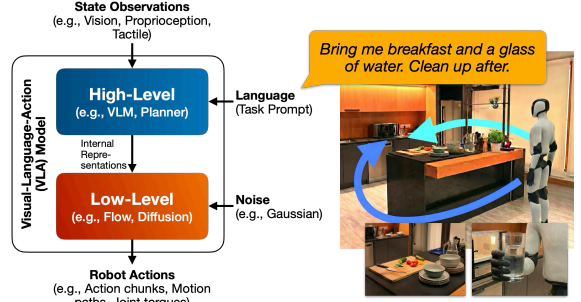


Figure 1: (Left) The prototypical generative VLA analyzed in this work. Given state observations, a task prompt, and a noise sample, the model outputs robot actions. Recent VLAs are structured into a high-level planner and a low-level action head, but part of our theory also applies to those that do not have this explicit structure (e.g., RDT [8]). (Right) An example where a robot is given a long-horizon task that involves multi-modality and precision.

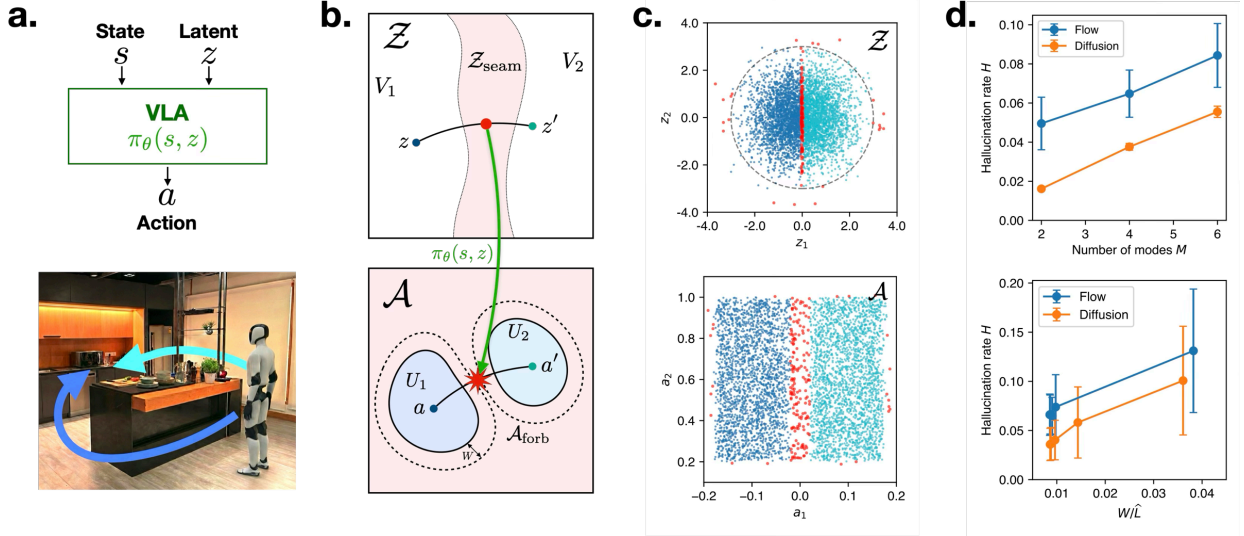


Figure 2: **Topological barrier for latent-variable VLA policies.** (a) We study generative VLAs whose action head is a conditional latent-variable policy that maps a task-relevant state (or history of observations) and latent noise z to a continuous action (or action chunk). In the illustrated navigation example, reaching the microwave requires going *left* or *right* around the kitchen island, inducing two qualitatively distinct modes of valid behaviors. (b) Schematic of the topological barrier (Lemma 9). The valid actions (bottom panel) decompose into disconnected components U_1 and U_2 (e.g., left vs. right), separated by a forbidden region $\mathcal{A}_{\text{forb}}$. If $\pi_\theta(s, \cdot)$ is continuous and maps $z \mapsto a \in U_1$ and $z' \mapsto a' \in U_2$, then any continuous latent path between z and z' must cross an *open seam* $\mathcal{Z}_{\text{seam}} = \pi_\theta(s, \cdot)^{-1}(\mathcal{A}_{\text{forb}})$, implying non-zero hallucination probability. (c) Diffusion model trained on bimodal action data: red points in \mathcal{Z} (top) lie on the seam and decode to forbidden actions in \mathcal{A} (bottom). See Appendix D.1 for details. (d) Empirical trends for flow matching and diffusion. Hallucination rates H can increase approximately linearly with the number of covered modes M (top) and grows with W/\hat{L} (bottom), consistent with Theorem 11 (\hat{L} is the numerically-estimated Lipschitz constant).

3 Low-Level Action Hallucinations

3.1 Topological Barrier for Multi-Mode Coverage

Recent VLAs and generative policies are often lauded for their ability to represent complex *multi-modal* action trajectories (e.g., “go left” or “go right” around an obstacle). However, experiments show these models still produce invalid actions despite significant training [10, 11, 13] or drop action modes [42]. Figure 2 provides a high-level overview of our theoretical results below that explains why this can occur.

Fix a physical state $s \in \mathcal{S}$ and instruction ℓ . We first consider situations where the valid actions at a fixed state decompose into two distinct safe ‘modes’, U_L and U_R (e.g., two inverse-kinematics branches, two grasp approach directions), separated by physically forbidden actions (e.g., joint-limit violation, infeasible contact).

Assumption 8. For a given state s , assume that the safe action set $\mathcal{A}_{\text{safe}}(s)$ has at least two disjoint, nonempty path-connected components U_L and U_R in the subspace topology of \mathcal{A} . Also assume that the forbidden region $\mathcal{A}_{\text{forb}}(s)$ is open in \mathcal{A} and has nonempty interior.

In this setting, topology dictates that a latent action head that attempts to cover both modes must hallucinate.

Lemma 9 (Topological Barrier). Suppose Assumption 8 holds and there exist $z_L, z_R \in \mathcal{Z}$ such that $\pi_\theta(s, z_L) \in U_L$ and $\pi_\theta(s, z_R) \in U_R$. Define the seam set, $\mathcal{Z}_{\text{seam}}(s) := \{z \in \mathcal{Z} : \pi_\theta(s, z) \in \mathcal{A}_{\text{forb}}(s)\}$. Then $\mathcal{Z}_{\text{seam}}(s)$ is nonempty and open in \mathcal{Z} . The hallucination probability at s is strictly positive, $H_\theta(s) = \Pr_{z \sim p_Z} [z \in \mathcal{Z}_{\text{seam}}(s)] > 0$.

Lemma 9 (proof in Appendix A.1) translates a geometric concept in deep generative modeling (e.g., [29, 30, 28]) to robotics—if there are distinct modes of valid behaviors at a given state, then any generative policy that is smooth in its latent input must create a “seam” of *in-between* latents that decode to *in-between* actions. The policy cannot assign probability mass to both modes without also assigning probability mass to the invalid or unsafe actions between them.

Next, we derive a quantitative lower bound in a multi-mode setting (≥ 2). Assumption 10 below extends the previous setup to one where the valid action set $\mathcal{A}_{\text{safe}}(s)$ splits into M disconnected modes U_1, U_2, \dots, U_M . These modes in action space are separated by at least a distance $2W$ with a forbidden buffer of thickness W around each mode.

Assumption 10. For a given state s , we assume that the safe set decomposes into $M \geq 2$ nonempty, pairwise-disjoint, closed, path-connected components $\mathcal{A}_{\text{safe}}(s) = \bigsqcup_{i=1}^M U_i$. Assume there exists $W > 0$ such that $\text{dist}(U_i, U_j) :=$

$\inf_{a \in U_i, a' \in U_j} \|a - a'\| \geq 2W$ for all $i \neq j$, and for each i , the W -neighborhood of U_i outside U_i itself is forbidden: $\{a \in \mathcal{A} : 0 < \text{dist}(a, U_i) < W\} \subseteq \mathcal{A}_{\text{forb}}(s)$.

In the common Gaussian latent setting, we can lower-bound the hallucination rate of smooth policies that are locally Lipschitz in z .

Theorem 11 (Isoperimetric lower bound on action hallucination). *Fix a state s satisfying Assumption 10. Let $Z \sim \mathcal{N}(0, I_m)$ and fix a radius $R > 0$. Assume that the latent-to-action head $z \mapsto \pi_\theta(s, z)$ is L -Lipschitz on the typical-latent ball $B_R := \{z \in \mathbb{R}^m : \|z\| \leq R\}$, i.e., $\|\pi_\theta(s, z) - \pi_\theta(s, z')\| \leq L\|z - z'\| \forall z, z' \in B_R$ and $L > 0$. Let $\epsilon := W/L$. For each safe mode U_i , define the latent preimage $V_i := \pi_\theta(s, \cdot)^{-1}(U_i)$ and the in-ball mass $p_i^{(R)} := \Pr[Z \in V_i \cap B_R]$. Let $q(R) = \Pr[\|Z\| > R]$. Then the hallucination probability at s satisfies*

$$H_\theta(s) \geq \sum_{i=1}^M \left[\Phi\left(\Phi^{-1}(p_i^{(R)}) + \epsilon\right) - p_i^{(R)} \right] - q(R), \quad (1)$$

where Φ is the CDF of the standard normal distribution.

Compared to Lemma 9, Theorem 11 provides a quantitative lower bound that reveals key factors that influence the action hallucination rate. As before, the problem is interpolation between the M modes. The more smoothly the policy varies with the latent, the more probability mass leaks into the forbidden seam. In addition to the number of modes M , a key ratio to note is $\epsilon = W/L$. W measures how wide the unsafe gap is in action space, and L measures how quickly actions can change as we adjust the latent z . If the model is very smooth in the latent space, then it must transition gradually, and a larger set of latents produce intermediate invalid actions. The main idea underlying the proof (Appendix A.2) is to apply Gaussian isoperimetry to lower bound the mass of disjoint latent ‘‘halos’’ of radius $\epsilon = W/L$ around each safe-mode set.

Implications for VLAs. Our analysis reveals a tension between *diversity* and *safety*. Datasets can be multi-modal (e.g., distinct grasp types or approach trajectories) and a low-level continuous policy trained to cover all M modes equally faces a geometric dilemma: (i) **Accept Hallucination:** To cover all diverse modes, the policy is geometrically required to expose significant Gaussian surface area to the forbidden regions, resulting in invalid ‘‘interpolated’’ actions; or (ii) **Mode Collapse:** To reduce the hallucination rate (minimize H_θ), the policy can assign very little mass to some modes or drop modes entirely (reduce M).

Crucially, this dilemma is a geometric consequence and does *not* disappear with better optimization or more data. One theoretical solution is to break the continuity assumption: generative action heads can employ *hybrid* designs that use discrete decisions to switch between modes (e.g., discrete tokens [43, 44, 45], diffusion options [46], or mixture-of-experts (MoE) gating [47]). Recent work provides suggestive empirical support for this prescription; VFP [10] uses a MoE flow decoder to encourage mode-specific action generation, while Hybrid Diffusion Planner [45] jointly samples discrete plan tokens and continuous trajectories to reduce long-horizon mode confusion. Both lead to better performance. In VLAs, the VLM/high-level planner can sample the mode before invoking the generative action head. However, this shifts the burden of hallucination avoidance to the planner (see Sec. 4). Theorem 11 also indicates that smoothness is a ‘‘double-edged sword’’ for contemporary models: on one hand, smoothness is generally encouraged in (learnt) policies as it is associated with more stable training [28] and robot behavior—we usually prefer the case that similar z imply similar actions. On the other hand, smoothness likely has a *negative* effect on action hallucination; all else being equal, in (1), each term $\Phi(\Phi^{-1}(p_i^{(R)}) + \epsilon) - p_i^{(R)}$ is increasing in $\epsilon = W/L$.

3.2 Precision Barrier for Contact Tasks

Let us now shift our attention from multiple modes to the complementary regime of precision and contact-rich tasks. Once contact occurs, rigid-body non-penetration, admissible contact modes, and practical limits such as maximum contact wrench induce additional state-dependent constraints on which actions are physically allowed. The set of admissible actions forms a thin tube around a lower-dimensional set in action space. Here, we revisit this *precision-barrier* from classical robotics [23] and we show that, as tolerance around the tube shrinks, any policy with a *smooth, full-dimensional* action density is almost guaranteed to hallucinate actions (See Fig. 3 for an overview).

We model ideal contact configurations as a state-dependent k -dimensional submanifold $\mathcal{M}(s)$:

Definition 12. *Let $\mathcal{M}(s) \subset \mathcal{A}$ be a compact C^1 submanifold of dimension $k < d$. For $\delta > 0$, define the δ -tube around $\mathcal{M}(s)$ by $\mathcal{M}_\delta(s) := \{a \in \mathcal{A} : \text{dist}(a, \mathcal{M}(s)) \leq \delta\}$, where $\text{dist}(a, \mathcal{M}) = \inf_{x \in \mathcal{M}} \|a - x\|$. For a state s , suppose the safe terminal actions satisfy $\mathcal{A}_{\text{safe}}(s; \delta) \subseteq \mathcal{M}_\delta(s)$ for a task-specific tolerance δ . Define the δ -tolerant success $S_\theta(s; \delta) := \Pr[a \in \mathcal{A}_{\text{safe}}(s; \delta)]$, and hallucination probabilities, $H_\theta(s; \delta) := \Pr[a \notin \mathcal{A}_{\text{safe}}(s; \delta)] = 1 - S_\theta(s; \delta)$.*

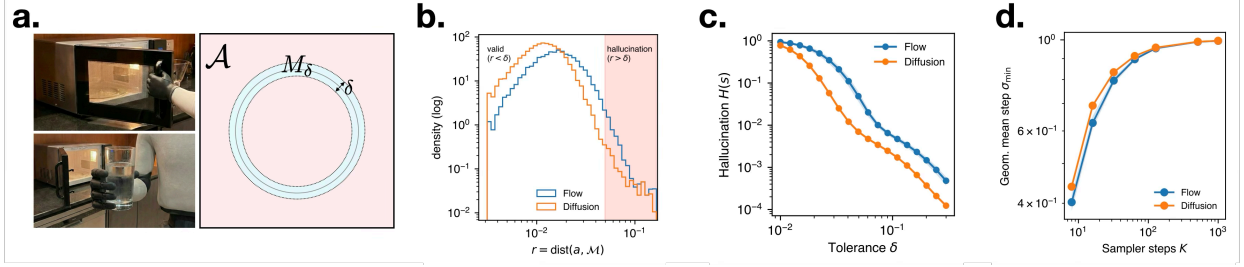


Figure 3: **Precision barrier for contact-rich tasks.** (a) Many manipulation tasks (e.g., grasping, peg-in-hole, handling tools / articulated / deformable objects) require high precision in that valid actions concentrate near a lower-dimensional feasible set. We model this as a k -dimensional manifold $\mathcal{M} \subset \mathcal{A}$ with tolerance tube $\mathcal{M}_\delta = \{a : \text{dist}(a, \mathcal{M}) \leq \delta\}$ (schematic). (b) Empirical distribution of distances $r = \text{dist}(a, \mathcal{M})$ for samples from flow matching and diffusion (log scales). The shaded region $r > \delta$ corresponds to action hallucinations. See Appendix D.2 for experiment details. (c) Action hallucination rate $H(s; \delta) = \Pr[r > \delta]$ versus tolerance δ (log-log). Tightening tolerance sharply increases hallucinations, consistent with our precision barrier (Lemma 13) that shows maintaining low hallucination at small δ requires increasingly concentrated mass near \mathcal{M} . (d) The geometric mean of per-step minimum singular values increases toward 1 as the number of sampler steps K grows, indicating that the necessary overall contraction can be distributed across many mild refinement steps rather than a single severe collapse (Theorem 14 and Corollary 15).

We fix a state s and write $\mathcal{M} := \mathcal{M}(s)$ and $\mathcal{M}_\delta := \mathcal{M}_\delta(s)$. Assume that the dimensionality of the latent code z is the same as the action, $m = d$ (as is the case in flow-matching and DDIM models). Below, we show that hitting a low-dimensional contact manifold requires the action distribution to concentrate its probability density.

Lemma 13 (Precision Barrier). *Fix a state s and adopt Definition 12. Assume that the induced action law $\mu_\theta(\cdot | s)$ is absolutely continuous with respect to d -dimensional Lebesgue measure on \mathcal{A} , with density $p(\cdot | s)$. Then, there exist constants $C_{\mathcal{M}} > 0$ and $\bar{\delta} > 0$ (depending only on \mathcal{M}) such that for all $0 < \delta \leq \bar{\delta}$, $S_\theta(s; \delta) \leq C_{\mathcal{M}} \delta^{d-k} \cdot \text{ess sup}_{a \in \mathcal{M}_\delta} p(a | s)$, and hence*

$$H_\theta(s; \delta) \geq 1 - C_{\mathcal{M}} \delta^{d-k} \cdot \text{ess sup}_{a \in \mathcal{M}_\delta} p(a | s). \quad (2)$$

Lemma 13 (proof in Appendix B.1) captures a source of action hallucination that is *distinct* from the topological barrier in Section 3.1. Even when the valid action set is connected (a single contact manifold), the policy needs to generate probability densities scaling as $O(\delta^{-(d-k)})$ inside the δ -tube around \mathcal{M} . This becomes more challenging as the tolerance δ shrinks or the codimension $(d - k)$ increases. The following theorem shows how a policy can supply this extreme density.

Theorem 14 (The Precision Trilemma: Collapse, Fold, or Hallucinate). *Let $m = d$ and let the action be generated by $a = F(z)$ where $Z \sim p_Z$. Assume F is C^1 on an open set $U \subseteq \mathcal{Z}$ containing the support of p_Z , with bounded latent density $\rho_Z(z) \leq \rho_Z^{\max}$. Define the active latent set as $Z_\delta := F^{-1}(\mathcal{M}_\delta) \cap U$. Define local folding and local conditioning restricted to this active set: $N_\delta := \text{ess sup}_{a \in \mathcal{M}_\delta} \#\{z \in Z_\delta : F(z) = a\}$, and $\sigma_*(\delta) := \text{ess inf}_{z \in Z_\delta} \sigma_{\min}(J_F(z))$, where $J_F(z)$ is the Jacobian of F and $\sigma_{\min}(J_F(z))$ its smallest singular value. Assume F is finite-to-one on Z_δ (i.e., $N_\delta < \infty$) and $\sigma_*(\delta) > 0$. Then the induced action distribution admits a density on \mathcal{M}_δ and the hallucination rate satisfies $H_\theta(s; \delta) \geq 1 - C_{\mathcal{M}} \delta^{d-k} N_\delta \rho_Z^{\max} \sigma_*(\delta)^{-d}$. If the policy achieves a target hallucination level $H_\theta(s; \delta) \leq \eta$ for some $\eta \in (0, 1)$, then the generator must satisfy*

$$\underbrace{N_\delta}_{\text{Fold}} \cdot \underbrace{\sigma_*(\delta)^{-d}}_{\text{Collapse}} \geq \frac{1 - \eta}{C_{\mathcal{M}} \rho_Z^{\max}} \delta^{-(d-k)}. \quad (3)$$

Hence, as precision tightens ($\delta \rightarrow 0$), any policy that maintains $H_\theta(s; \delta) \leq \eta$ must either fold space ($N_\delta \rightarrow \infty$) or collapse volume locally ($\sigma_*(\delta) \rightarrow 0$).

Theorem 14 (proof in Appendix B.2) shows that near the tube, the induced action density satisfies $p(a | s) \lesssim N_\delta \cdot \rho_Z^{\max} \cdot \sigma_*(\delta)^{-d}$ so the two architectural mechanisms to increase density are: (i) **Collapse** (Jacobian contraction): make $\sigma_*(\delta)$ small so F compresses latent volume into a tiny region of action space; or (ii) **Fold** (many-to-one decoding): make N_δ large so that many disjoint latent regions decode to the same actions. If neither occurs, the policy cannot place enough mass in the tube and will hallucinate actions. In short, as $\delta \rightarrow 0$, the generative policy must either collapse, fold, or hallucinate.

Modern VLAs often use flow-matching to generate actions. In theory, these are diffeomorphic generators with invertible steps so folding is not possible ($N_\delta = 1$) and meeting the density requirement at tight tolerances requires Jacobian

collapse. These methods apply a sequence of “refinement” (or denoising) steps and Corollary 15 below (proof in Appendix B.3) shows that to maintain a fixed hallucination rate at increasingly tight tolerances, a flow-like policy must either accumulate sufficient latent-space contraction across its K refinement steps or allow individual steps to become increasingly ill-conditioned.

Corollary 15 (K -step precision tradeoff). *Assume the decoder is a K -step composition $F^{(K)} = \Phi_{K-1} \circ \dots \circ \Phi_0$, where each Φ_t is a C^1 diffeomorphism and there exist constants $\lambda_t > 0$ such that $\sigma_{\min}(J\Phi_t(z)) \geq \lambda_t$ for all z . Let $\sigma_*(\delta) \geq \inf_{z \in \mathcal{Z}_\delta} \sigma_{\min}(JF^{(K)}(z)) \geq \prod_{t=0}^{K-1} \lambda_t$. Then, for all $0 < \delta \leq \bar{\delta}$, $H_\theta^{(K)}(s; \delta) \geq 1 - C_{\mathcal{M}\rho_Z^{\max}} \left(\prod_{t=0}^{K-1} \lambda_t \right)^{-d} \delta^{d-k}$. In particular, if $\lambda_t \geq \lambda \in (0, 1)$ for all t , then a necessary condition to bound the hallucination rate $H_\theta^{(K)}(s; \delta) \leq \eta \in (0, 1)$ is $K \geq \frac{1}{d \log(1/\lambda)} \left[(d-k) \log \frac{1}{\delta} + \log \frac{1-\eta}{C_{\mathcal{M}\rho_Z^{\max}}} \right]$.*

Implications for VLAs. In this regime of contact-rich tasks, a policy *should* concentrate probability mass onto the safe action manifold rather than preserve spurious variance that gives rise to action hallucinations. However, there is a cost. Theorem 14 shows that achieving this requires either Jacobian collapse or folding. Both make the latent space a poor coordinate system for optimization. A possible path around the precision barrier is to *project* the VLA’s proposed action back onto the task’s feasible contact manifold (e.g., via a low-level controller, or external sensing like tactile feedback) or *parameterize* the manifold (e.g., an atlas of local charts [48] or kinematically-valid trajectories [49]) so decoded actions stay on-manifold by construction.

Corollary 15 suggests the iterative nature of modern flow and diffusion policies is not solely about sampling from complex action distributions, but rather, about decomposing an effectively singular projection into a product of gentle, well-behaved steps. The dependence on δ enters only through a $\log(1/\delta)$ factor, so the required number of refinement steps grows only logarithmically with tolerance. Interestingly, very recent large-scale empirical evidence [42] on benchmarks supports this view and suggests that the advantage of diffusion/flow-style policies on challenging contact-rich tasks is strongly associated with iterative computation and stochasticity injection, rather than distribution learning. Our theory serves to explain these empirical findings.

4 Long-Horizon Plan Hallucinations

This section builds on the previous analysis of one-step action generation and extends it to long-horizon goal achievement. We now move one layer up to the VLM/VLA planner and develop a theoretical framework that complements empirical findings showing that VLMs/VLAs suffer sharp performance degradation on long-horizon tasks (e.g., [14, 50, 12, 39]) and recent explorations into test-time compute (e.g., [39, 40]).

We begin by fixing a task instance I with deterministic dynamics \mathcal{T} and defining time-bounded backward-reachable sets, $\Sigma_0 := \mathcal{G}$, $\Sigma_t := \{s \in \mathcal{S} : \exists a \in \mathcal{A} \text{ s.t. } f_{\text{phys}}(s, a) = 1 \text{ and } \mathcal{T}(s, a) \in \Sigma_{t-1}\}$ for $t \geq 1$. Thus, $s \in \Sigma_t$ means that from state s there exists a physically-valid action that lands in a state from which the goal is reachable in t further steps. For a state s and remaining horizon $t \geq 1$ define the *progress set*, $\mathcal{A}_{\text{prog}}(s, t) := \{a \in \mathcal{A} : f_{\text{phys}}(s, a) = 1 \text{ and } \mathcal{T}(s, a) \in \Sigma_{t-1}\}$. By construction, $s \in \Sigma_t$ if and only if $\mathcal{A}_{\text{prog}}(s, t) \neq \emptyset$, and $\mathcal{A}_{\text{prog}}(s, t) \subseteq \mathcal{A}_{\text{safe}}(s)$, i.e., progress actions are a subset of safe actions.

Lemma 16 (Horizon Barrier). *Let $(S_t)_{t=0}^T$ be the rollout from s_0 . Define $p_t(s) := \Pr_{Z \sim p_Z} [\pi_\theta(s, Z) \in \mathcal{A}_{\text{prog}}(s, t)]$ and $\gamma_t := \sup_{s \in \Sigma_t} p_t(s)$. Then the rollout success probability factorizes and is upper bounded by $\Pr[f_{\text{plan}}(s_0, \tau_\theta(s_0, Z_{0:T-1})) = 1] \leq \prod_{t=1}^T \gamma_t$. Hence, $H_{\pi_\theta}^{\text{plan}}(I) \geq 1 - \prod_{t=1}^T \gamma_t$. In particular, if $\gamma_t \leq \gamma < 1$ for all t , then $\Pr[f_{\text{plan}}(s_0, \tau_\theta) = 1] \leq \gamma^T$ and $H_{\pi_\theta}^{\text{plan}}(I) \geq 1 - \gamma^T$.*

Lemma 16 (proof in Appendix C.1) formalizes the horizon barrier as a *compounding reachability bottleneck*. The idea is intuitive and well-known in robotics [17]: a length- T valid rollout requires sampling a progress action at every step, so success is a product of conditional progress factors. Even if each γ_t is only slightly below one, their product decays rapidly with horizon. This connects directly to the topological and precision barriers since both reduce per-step progress probability and the deficit compounds with T (also see the discussion in Appendix C.6 on action chunking).

Now suppose that a VLA can expend *test-time compute* to *propose* and *verify* candidates or continuations, as in sampling, beam/tree search, or using simulator/world-model rollouts. Let \mathcal{P}_I be a measurable space of complete grounded candidate continuations for instance I ; each $\tau \in \mathcal{P}_I$ induces an action sequence, so $f_{\text{plan}}(s_0, \tau; \mathcal{G})$ is well-defined. Define the valid set $V := \{\tau \in \mathcal{P}_I : f_{\text{plan}}(s_0, \tau; \mathcal{G}) = 1\}$. We study a *verification-guided planner* that runs for at most q rounds. At round j , based on its search history, it chooses a proposal distribution Q_j over \mathcal{P}_I , samples $\tau_j \sim Q_j$, queries a randomized verifier $\tilde{f}_j(\tau_j)$, and outputs the first accepted candidate; if no candidate is accepted in q

rounds, it abstains and outputs \perp . We assume verifier errors are uniformly bounded: given any history and proposed τ , invalid candidates are accepted with probability at most ε_{fp} , and valid candidates are accepted with probability at least $c := 1 - \varepsilon_{\text{fn}}$.

Define hallucination and abstention probabilities, $H(I) := \Pr[\hat{\tau} \neq \perp \wedge \hat{\tau} \notin V]$ and $A(I) := \Pr[\hat{\tau} = \perp]$. The valid-output probability is $S(I) = 1 - A(I) - H(I)$. Plan hallucination here differs slightly from Lemma 16 because the planner may abstain. We focus on the design of (α, β) -reliable VLAs:

Definition 17 ((α, β) -reliability). *Fix $\alpha, \beta \in [0, 1]$ with $\alpha + \beta \leq 1$. We say the planner is (α, β) -reliable on instance I if $H(I) \leq \alpha$ and $A(I) \leq \beta$. Hence, an (α, β) -reliable planner outputs a valid plan with probability at least $S(I) \geq 1 - \alpha - \beta$.*

Let C_{j-1} be the event that the planner reaches round j . Define the round- j conditional valid mass by $\rho_j := \Pr[\tau_j \in V \mid C_{j-1}] = \mathbb{E}[Q_j(V) \mid C_{j-1}]$, with the convention $\rho_j = 0$ if $\Pr[C_{j-1}] = 0$. We refer to $(\rho_j)_{j=1}^q$ as the planner’s amplification schedule.

Lemma 18 (Reliability search-budget window). *Consider any verification-guided planner with budget q , verifier error rates $(\varepsilon_{\text{fp}}, \varepsilon_{\text{fn}})$, and amplification schedule $(\rho_j)_{j=1}^q$. Let $c := 1 - \varepsilon_{\text{fn}}$. Then $H(I) \leq \varepsilon_{\text{fp}} \sum_{j=1}^q \Pr[C_{j-1}](1 - \rho_j) \leq q\varepsilon_{\text{fp}}$ and $A(I) \leq \prod_{j=1}^q (1 - c\rho_j)$. Consequently, the planner is certified as (α, β) -reliable whenever $\varepsilon_{\text{fp}} \sum_{j=1}^q \Pr[C_{j-1}](1 - \rho_j) \leq \alpha$ and $\prod_{j=1}^q (1 - c\rho_j) \leq \beta$. The simpler sufficient certificate $q\varepsilon_{\text{fp}} \leq \alpha$ and $\prod_{j=1}^q (1 - c\rho_j) \leq \beta$ also certifies (α, β) -reliability.*

Lemma 18 separates verifier-limited and planner-limited effects. Each query creates a chance to accept a valid plan, but also increases the worst-case (upper-bounded) cumulative risk of a hallucination. Thus test-time compute is useful only if the proposal mechanism increases ρ_j fast enough before the certified hallucination budget is exhausted. A natural follow-up question is how fast a planner needs to grow ρ_j ? The following theorem provides an answer for long horizon tasks.

Theorem 19 (Amplification-rate to beat the horizon barrier). *Consider the planner above, with amplification schedule $(\rho_j)_{j=1}^q$. Any (α, β) -reliable planner must satisfy $\sum_{j=1}^q \Pr[C_{j-1}]\rho_j \geq 1 - \alpha - \beta$. Assume an exponentially small initial valid mass $\rho_1 \leq \gamma^T$ for some $\gamma \in (0, 1)$. Then (i) **Polynomial amplification is insufficient.** If $\rho_j \leq \rho_1 j^p$ for some fixed $p \geq 0$, then meeting the necessary condition requires $q \geq \left(1 + \frac{(p+1)(1-\alpha-\beta)}{\gamma^T}\right)^{1/(p+1)} - 1$. For fixed $p, \gamma \in (0, 1)$, and nontrivial reliability target $1 - \alpha - \beta > 0$, this lower bound grows exponentially in T ; (ii) **Geometric amplification is sufficient, if within the verifier budget.** Assume $c := 1 - \varepsilon_{\text{fn}} > 0$, $\beta \in (0, 1)$, and $\rho_j \geq \min\{1, \rho_1 r^{j-1}\}$ for some $r > 1$. Then $q\varepsilon_{\text{fp}} \leq \alpha$ and $\sum_{j=1}^q \min\{1, \rho_1 r^{j-1}\} \geq c^{-1} \log(1/\beta)$ certify (α, β) -reliability. In the unsaturated regime $\rho_1 r^{q-1} \leq 1$, the second condition becomes $\rho_1 \frac{r^q - 1}{r - 1} \geq c^{-1} \log(1/\beta)$ and it suffices that $q \geq \log_r \left(1 + \frac{(r-1)c^{-1} \log(1/\beta)}{\rho_1}\right)$. Thus, for fixed $r > 1, c > 0$, and $\beta \in (0, 1)$, the geometric cumulative-mass condition is achieved at $q = \Theta(\log 1/\rho_1)$ rounds. If $\rho_1 \asymp \gamma^T$, this becomes $q = \Theta(T)$.*

Theorem 19 highlights a certificate-level feasibility constraint. When the horizon barrier makes the initial valid mass small, amplification that grows only polynomially with the number of rounds (e.g., simple accept/reject) cannot accumulate enough valid mass without exponentially many queries. At the same time, Lemma 18 gives the sufficient hallucination certificate $q\varepsilon_{\text{fp}} \leq \alpha$. If ε_{fp} is bounded away from zero, the certificate window can close for large T . In contrast, geometric amplification grows valid mass multiplicatively and can reach the abstention threshold quickly enough.

Implications for VLAs. Our analysis above provides us with key takeaways. First, long-horizon planning is difficult because success is a product of conditional progress factors. This problem has been long recognized in robotics and remains applicable to contemporary VLAs. A practical (and historically natural) way to address the horizon barrier is to leverage hierarchy, e.g., verify and replan at intermediate semantic or skill boundaries, which turns one length- T rare-event into many shorter-horizon problems. A complementary approach is to verify actions/plans. The verification-guided framework in Lemma 18 clarifies what test-time compute can and cannot buy with noisy verifiers. The prescriptive message is that high-level VLM/VLA planners should not treat verification as a binary filter on complete trajectories (more in Appendix C.3). They should use *feedback* to reshape Q_j so that ρ_j grows *multiplicatively*. In robotics, gains often come from exploiting *structure*; planners use verifier tests/scoring (e.g., partial constraints or intermediate progress tests) to prune large families of continuations at once (e.g., via tree search). See Appendix C.7 for a short but more formal discussion. These methodologies have been recently adopted in LLMs (e.g., [51, 52, 53]) and are finding their way into VLAs [40, 41], and our theory makes clear when and why search is important.

5 Conclusions, Discussion, and Future Work

Taken together, our results suggest that robust VLAs are unlikely to emerge from scale alone. A core challenge is *structural*: hallucination-free and successful behavior lives on disconnected and thin subsets of action space, and long horizons turn small local errors into global failures. Our analysis points to design principles more specific than “scale the data”, “increase the number of layers”, or “add a verifier”: we should design VLA systems so that test-time computation is spent on multiplicative amplification of *valid* behavior under controlled verification error, and *structure* robot architectures to make that amplification possible.

Limitations and future work. We view this work as a step toward a broader theory of VLAs and other RFMs such as World Action Models. Extending our theory to encompass perception, memory, and stochasticity is a natural step forward. Our verification-guided planning model also simplifies planning and verification; richer models could tighten amplification requirements and yield sharper algorithmic guidance. Beyond verification, future work can examine other reasoning approaches [54, 6, 49]. Finally, it would be interesting to extend our theory towards task distributions and to training/test-time interventions that reduce hallucinations. Progress along these lines can guide the development of next-generation VLAs that are not only more capable, but more *trustworthy*.

References

- [1] Brianna Zitkovich, Tianhe Yu, Sichun Xu, Peng Xu, Ted Xiao, Fei Xia, Jialin Wu, Paul Wohlhart, Stefan Welker, Ayzaan Wahid, Quan Vuong, Vincent Vanhoucke, Huong Tran, Radu Soricut, Anikait Singh, Jaspiar Singh, Pierre Sermanet, Pannag R. Sanketi, Grecia Salazar, Michael S. Ryoo, Krista Reymann, Kanishka Rao, Karl Pertsch, Igor Mordatch, Henryk Michalewski, Yao Lu, Sergey Levine, Lisa Lee, Tsang-Wei Edward Lee, Isabel Leal, Yuheng Kuang, Dmitry Kalashnikov, Ryan Julian, Nikhil J. Joshi, Alex Irpan, Brian Ichter, Jasmine Hsu, Alexander Herzog, Karol Hausman, Keerthana Gopalakrishnan, Chuyuan Fu, Pete Florence, Chelsea Finn, Kumar Avinava Dubey, Danny Driess, Tianli Ding, Krzysztof Marcin Choromanski, Xi Chen, Yevgen Chebotar, Justice Carbajal, Noah Brown, Anthony Brohan, Montserrat Gonzalez Arenas, and Kehang Han. Rt-2: Vision-language-action models transfer web knowledge to robotic control. In Jie Tan, Marc Toussaint, and Kourosh Darvish, editors, *Proceedings of The 7th Conference on Robot Learning*, volume 229 of *Proceedings of Machine Learning Research*, pages 2165–2183. PMLR, 06–09 Nov 2023.
- [2] Moo Jin Kim, Karl Pertsch, Siddharth Karamcheti, Ted Xiao, Ashwin Balakrishna, Suraj Nair, Rafael Rafailov, Ethan Foster, Grace Lam, Pannag Sanketi, Quan Vuong, Thomas Kollar, Benjamin Burchfiel, Russ Tedrake, Dorsa Sadigh, Sergey Levine, Percy Liang, and Chelsea Finn. Openvla: An open-source vision-language-action model, 2024.
- [3] Kevin Black, Noah Brown, Danny Driess, Adnan Esmail, Michael Equi, Chelsea Finn, Niccolo Fusai, Lachy Groom, Karol Hausman, Brian Ichter, et al. π_0 : A vision-language-action flow model for general robot control. *arXiv preprint arXiv:2410.24164*, 2024.
- [4] NVIDIA, :, Johan Bjorck, Fernando Castañeda, Nikita Cherniadev, Xingye Da, Runyu Ding, Linxi "Jim" Fan, Yu Fang, Dieter Fox, Fengyuan Hu, Spencer Huang, Joel Jang, Zhenyu Jiang, Jan Kautz, Kaushil Kundalia, Lawrence Lao, Zhiqi Li, Zongyu Lin, Kevin Lin, Guilin Liu, Edith Llontop, Loic Magne, Ajay Mandlekar, Avnish Narayan, Soroush Nasiriany, Scott Reed, You Liang Tan, Guanzhi Wang, Zu Wang, Jing Wang, Qi Wang, Jiannan Xiang, Yuqi Xie, Yinzhen Xu, Zhenjia Xu, Seonghyeon Ye, Zhiding Yu, Ao Zhang, Hao Zhang, Yizhou Zhao, Ruijie Zheng, and Yuke Zhu. Gr00t n1: An open foundation model for generalist humanoid robots, 2025.
- [5] Physical Intelligence, Kevin Black, Noah Brown, James Darpinian, Karan Dhabalia, Danny Driess, Adnan Esmail, Michael Equi, Chelsea Finn, Niccolo Fusai, et al. $\pi_{0.5}$: a vision-language-action model with open-world generalization. *arXiv preprint arXiv:2504.16054*, 2025.
- [6] Jason Lee, Jiafei Duan, Haoquan Fang, Yuquan Deng, Shuo Liu, Boyang Li, Bohan Fang, Jieyu Zhang, Yi Ru Wang, Sangho Lee, Winson Han, Wilbert Pumacay, Angelica Wu, Rose Hendrix, Karen Farley, Eli VanderBilt, Ali Farhadi, Dieter Fox, and Ranjay Krishna. Molmoact: Action reasoning models that can reason in space, 2025.
- [7] Cheng Chi, Zhenjia Xu, Siyuan Feng, Eric Cousineau, Yilun Du, Benjamin Burchfiel, Russ Tedrake, and Shuran Song. Diffusion policy: Visuomotor policy learning via action diffusion. *The International Journal of Robotics Research*, 44(10-11):1684–1704, 2025.
- [8] Songming Liu, Lingxuan Wu, Bangguo Li, Hengkai Tan, Huayu Chen, Zhengyi Wang, Ke Xu, Hang Su, and Jun Zhu. RDT-1b: a diffusion foundation model for bimanual manipulation. In *The Thirteenth International Conference on Learning Representations*, 2025.

- [9] Qinglun Zhang, Zhen Liu, Haoqiang Fan, Guanghui Liu, Bing Zeng, and Shuaicheng Liu. Flowpolicy: Enabling fast and robust 3d flow-based policy via consistency flow matching for robot manipulation, 2024. URL <https://arxiv.org/abs/2412.04987>.
- [10] Xuanran Zhai, Qianyou Zhao, Qiaojun Yu, and Ce Hao. Vfp: Variational flow-matching policy for multi-modal robot manipulation, 2025.
- [11] Xiaobing Dai, Zewen Yang, Dian Yu, Fangzhou Liu, Hamid Sadeghian, Sami Haddadin, and Sandra Hirche. Safeflow: Safe robot motion planning with flow matching via control barrier functions, 2025.
- [12] Rui Yang, Hanyang Chen, Junyu Zhang, Mark Zhao, Cheng Qian, Kangrui Wang, Qineng Wang, Teja Venkat Koripella, Marziyeh Movahedi, Manling Li, Heng Ji, Huan Zhang, and Tong Zhang. Embodiedbench: Comprehensive benchmarking multi-modal large language models for vision-driven embodied agents. In *Forty-second International Conference on Machine Learning*, 2025.
- [13] Xiaogang Jia, Denis Blessing, Xinkai Jiang, Moritz Reuss, Atalay Donat, Rudolf Lioutikov, and Gerhard Neumann. Towards diverse behaviors: A benchmark for imitation learning with human demonstrations. In *The Twelfth International Conference on Learning Representations*, 2024.
- [14] Liu Dai, Haina Wang, Weikang Wan, and Hao Su. Manitaskgen: A comprehensive task generator for benchmarking and improving vision-language agents on embodied decision-making. 2025.
- [15] Tomas Lozano-Pérez. Spatial planning: A configuration space approach. *IEEE Transactions on Computers*, C-32(2):108–120, 1983.
- [16] D. Hsu, J.-C. Latombe, and R. Motwani. Path planning in expansive configuration spaces. In *Proceedings of International Conference on Robotics and Automation*, volume 3, pages 2719–2726, 1997.
- [17] Stéphane Ross and Drew Bagnell. Efficient reductions for imitation learning. In *Proceedings of the thirteenth international conference on artificial intelligence and statistics*, pages 661–668. JMLR Workshop and Conference Proceedings, 2010.
- [18] Lei Huang, Weijiang Yu, Weitao Ma, Weihong Zhong, Zhangyin Feng, Haotian Wang, Qianglong Chen, Weihua Peng, Xiaocheng Feng, Bing Qin, and Ting Liu. A survey on hallucination in large language models: Principles, taxonomy, challenges, and open questions. *ACM Trans. Inf. Syst.*, 43(2), January 2025. ISSN 1046-8188.
- [19] Sheng Liu, Haotian Ye, and James Zou. Reducing hallucinations in large vision-language models via latent space steering. In *The Thirteenth International Conference on Learning Representations*, 2025.
- [20] Ziwei Xu, Sanjay Jain, and Mohan Kankanhalli. Hallucination is inevitable: An innate limitation of large language models, 2025.
- [21] Adam Tauman Kalai and Santosh S. Vempala. Calibrated language models must hallucinate. In *Proceedings of the 56th Annual ACM Symposium on Theory of Computing (STOC)*, 2024.
- [22] Ziwei Ji, Nayeon Lee, Rita Frieske, Tiezheng Yu, Dan Su, Yan Xu, Etsuko Ishii, Ye Jin Bang, Andrea Madotto, and Pascale Fung. Survey of hallucination in natural language generation. *ACM Comput. Surv.*, 55(12), March 2023. ISSN 0360-0300.
- [23] David Hsu, Jean-Claude Latombe, and Hanna Kurniawati. On the probabilistic foundations of probabilistic roadmap planning. *The International Journal of Robotics Research*, 25(7):627–643, 2006.
- [24] Matthew T Mason. Compliance and force control for computer controlled manipulators. *IEEE Transactions on Systems, Man, and Cybernetics*, 11(6):418–432, 1981.
- [25] Matthew Mason. The mechanics of manipulation. In *Proceedings. 1985 IEEE International Conference on Robotics and Automation*, volume 2, pages 544–548. IEEE, 1985.
- [26] Tomas Lozano-Perez, Matthew T Mason, and Russell H Taylor. Automatic synthesis of fine-motion strategies for robots. *The International Journal of Robotics Research*, 3(1):3–24, 1984.
- [27] Kris Hauser and Jean-Claude Latombe. Multi-modal motion planning in non-expansive spaces. *The International Journal of Robotics Research*, 29(7):897–915, 2010.
- [28] Antoine Salmona, Valentin De Bortoli, Julie Delon, and Agnes Desolneux. Can push-forward generative models fit multimodal distributions? *Advances in Neural Information Processing Systems*, 35:10766–10779, 2022.
- [29] Mahyar Khayatkhoei, Maneesh K. Singh, and Ahmed Elgammal. Disconnected manifold learning for generative adversarial networks. In Samy Bengio, Hanna Wallach, Hugo Larochelle, Kristen Grauman, Nicolò Cesa-Bianchi, and Roman Garnett, editors, *Advances in Neural Information Processing Systems 31*, pages 7354–7364. Curran Associates, Inc., 2018.

- [30] Ugo Tanielian, Thibaut Issenhuth, Elvis Dohmatob, and Jeremie Mary. Learning disconnected manifolds: a no GAN’s land. In Hal Daumé III and Aarti Singh, editors, *Proceedings of the 37th International Conference on Machine Learning*, volume 119 of *Proceedings of Machine Learning Research*, pages 9418–9427. PMLR, 13–18 Jul 2020.
- [31] Thibaut Issenhuth, Ugo Tanielian, Jeremie Mary, and David Picard. Unveiling the latent space geometry of push-forward generative models. In Andreas Krause, Emma Brunskill, Kyunghyun Cho, Barbara Engelhardt, Sivan Sabato, and Jonathan Scarlett, editors, *Proceedings of the 40th International Conference on Machine Learning*, volume 202 of *Proceedings of Machine Learning Research*, pages 14422–14444. PMLR, 23–29 Jul 2023.
- [32] George Papamakarios, Eric Nalisnick, Danilo Jimenez Rezende, Shakir Mohamed, and Balaji Lakshminarayanan. Normalizing flows for probabilistic modeling and inference. *Journal of Machine Learning Research*, 22(57):1–64, 2021.
- [33] Vincent Stimper, Bernhard Schölkopf, and Jose Miguel Hernandez-Lobato. Resampling base distributions of normalizing flows. In Gustau Camps-Valls, Francisco J. R. Ruiz, and Isabel Valera, editors, *Proceedings of The 25th International Conference on Artificial Intelligence and Statistics*, volume 151 of *Proceedings of Machine Learning Research*, pages 4915–4936. PMLR, 28–30 Mar 2022.
- [34] Sumukh K Aithal, Pratyush Maini, Zachary Chase Lipton, and J Zico Kolter. Understanding hallucinations in diffusion models through mode interpolation. In *The Thirty-eighth Annual Conference on Neural Information Processing Systems*, 2024. URL <https://openreview.net/forum?id=aNTnHBkw4T>.
- [35] John H Reif. Complexity of the mover’s problem and generalizations. In *20th Annual Symposium on Foundations of Computer Science (sfcs 1979)*, pages 421–427. IEEE Computer Society, 1979.
- [36] John Canny. *Complexity of Robot Motion Planning*. PhD thesis, MIT, 1988.
- [37] Herman Kahn and Theodore E Harris. Estimation of particle transmission by random sampling. *National Bureau of Standards applied mathematics series*, 12:27–30, 1951.
- [38] Reuven Y Rubinstein and Dirk P Kroese. *The cross-entropy method: a unified approach to combinatorial optimization, Monte-Carlo simulation and machine learning*. Springer Science & Business Media, 2004.
- [39] Jacky Kwok, Christopher Agia, Rohan Sinha, Matt Foutter, Shulu Li, Ion Stoica, Azalia Mirhoseini, and Marco Pavone. Robomonkey: Scaling test-time sampling and verification for vision-language-action models. In *Second Workshop on Out-of-Distribution Generalization in Robotics at RSS 2025*, 2025.
- [40] Jaesik Yoon, Hyeonsoo Cho, Doojin Baek, Yoshua Bengio, and Sungjin Ahn. Monte carlo tree diffusion for system 2 planning. In *Forty-second International Conference on Machine Learning*, 2025.
- [41] Zirui Zhao, Wee Sun Lee, and David Hsu. Large language models as commonsense knowledge for large-scale task planning. In *Proceedings of the 37th International Conference on Neural Information Processing Systems*, NIPS ’23, Red Hook, NY, USA, 2023. Curran Associates Inc.
- [42] Chaoyi Pan, Giri Anantharaman, Nai-Chieh Huang, Claire Jin, Daniel Pfrommer, Chenyang Yuan, Frank Permenter, Guannan Qu, Nicholas Boffi, Guanya Shi, and Max Simchowitz. Much ado about noising: Dispelling the myths of generative robotic control, 2025.
- [43] Michael Ahn, Anthony Brohan, Noah Brown, Yevgen Chebotar, Omar Cortes, Byron David, Chelsea Finn, Chuyuan Fu, Keerthana Gopalakrishnan, Karol Hausman, Alex Herzog, Daniel Ho, Jasmine Hsu, Julian Ibarz, Brian Ichter, Alex Irpan, Eric Jang, Rosario Jauregui Ruano, Kyle Jeffrey, Sally Jesmonth, Nikhil Joshi, Ryan Julian, Dmitry Kalashnikov, Yuheng Kuang, Kuang-Huei Lee, Sergey Levine, Yao Lu, Linda Luu, Carolina Parada, Peter Pastor, Jornell Quiambao, Kanishka Rao, Jarek Rettinghouse, Diego Reyes, Pierre Sermanet, Nicolas Sievers, Clayton Tan, Alexander Toshev, Vincent Vanhoucke, Fei Xia, Ted Xiao, Peng Xu, Sichun Xu, Mengyuan Yan, and Andy Zeng. Do as i can and not as i say: Grounding language in robotic affordances. In *arXiv preprint arXiv:2204.01691*, 2022.
- [44] Physical Intelligence, Ali Amin, Raichelle Aniceto, Ashwin Balakrishna, Kevin Black, Ken Conley, Grace Connors, James Darpinian, Karan Dhabalia, Jared DiCarlo, Danny Driess, Michael Equi, Adnan Esmail, Yunhao Fang, Chelsea Finn, Catherine Glossop, Thomas Godden, Ivan Goryachev, Lachy Groom, Hunter Hancock, Karol Hausman, Gashon Hussein, Brian Ichter, Szymon Jakubczak, Rowan Jen, Tim Jones, Ben Katz, Liyiming Ke, Chandra Kuchi, Marinda Lamb, Devin LeBlanc, Sergey Levine, Adrian Li-Bell, Yao Lu, Vishnu Mano, Mohith Mothukuri, Suraj Nair, Karl Pertsch, Allen Z. Ren, Charvi Sharma, Lucy Xiaoyang Shi, Laura Smith, Jost Tobias Springenberg, Kyle Stachowicz, Will Stoeckle, Alex Swerdlow, James Tanner, Marcel Torne, Quan Vuong, Anna Walling, Haohuan Wang, Blake Williams, Sukwon Yoo, Lili Yu, Ury Zhilinsky, and Zhiyuan Zhou. $\pi_{0.6}^*$: a vla that learns from experience, 2025.

- [45] Sigmund H Høeg, Aksel Vaaler, Chaoqi Liu, Olav Egeland, and Yilun Du. Hybrid diffusion for simultaneous symbolic and continuous planning. *IEEE Robotics and Automation Letters*, 2026.
- [46] Zeyu Feng, Hao Luan, Kevin Yuchen Ma, and Harold Soh. Diffusion meets options: Hierarchical generative skill composition for temporally-extended tasks. In *2025 IEEE International Conference on Robotics and Automation (ICRA)*, pages 10854–10860, 2025.
- [47] Ce Hao, Xuanran Zhai, Yaohua Liu, and Harold Soh. Abstracting robot manipulation skills via mixture-of-experts diffusion policies. In *The Fourteenth International Conference on Learning Representations*, 2026.
- [48] Léonard Jaillet and Josep M Porta. Path planning under kinematic constraints by rapidly exploring manifolds. *IEEE Transactions on Robotics*, 29(1):105–117, 2013.
- [49] NVIDIA, Yan Wang, Wenjie Luo, Junjie Bai, Yulong Cao, Tong Che, Ke Chen, Yuxiao Chen, Jenna Diamond, Yifan Ding, Wenhao Ding, Liang Feng, Greg Heinrich, Jack Huang, Peter Karkus, Boyi Li, Pinyi Li, Tsung-Yi Lin, Dongran Liu, Ming-Yu Liu, Langechuan Liu, Zhijian Liu, Jason Lu, Yunxiang Mao, Pavlo Molchanov, Lindsey Pavao, Zhenghao Peng, Mike Ranzinger, Ed Schmerling, Shida Shen, Yunfei Shi, Sarah Tariq, Ran Tian, Tilman Wekel, Xinshuo Weng, Tianjun Xiao, Eric Yang, Xiaodong Yang, Yurong You, Xiaohui Zeng, Wenyuan Zhang, Boris Ivanovic, and Marco Pavone. Alpamayo-r1: Bridging reasoning and action prediction for generalizable autonomous driving in the long tail, 2026.
- [50] Shiduo Zhang, Zhe Xu, Peiju Liu, Xiaopeng Yu, Yuan Li, Qinghui Gao, Zhaoye Fei, Zhangyue Yin, Zuxuan Wu, Yu-Gang Jiang, and Xipeng Qiu. Vlabench: A large-scale benchmark for language-conditioned robotics manipulation with long-horizon reasoning tasks. In *Proceedings of the IEEE/CVF International Conference on Computer Vision (ICCV)*, pages 11142–11152, October 2025.
- [51] Shunyu Yao, Dian Yu, Jeffrey Zhao, Izhak Shafran, Thomas L. Griffiths, Yuan Cao, and Karthik Narasimhan. Tree of thoughts: deliberate problem solving with large language models. In *Proceedings of the 37th International Conference on Neural Information Processing Systems, NIPS '23*, Red Hook, NY, USA, 2023. Curran Associates Inc.
- [52] Andy Zhou, Kai Yan, Michal Shlapentokh-Rothman, Haohan Wang, and Yu-Xiong Wang. Language agent tree search unifies reasoning acting and planning in language models, 2023.
- [53] Charlie Snell, Jaehoon Lee, Kelvin Xu, and Aviral Kumar. Scaling llm test-time compute optimally can be more effective than scaling model parameters, 2024.
- [54] Michał Zawalski, William Chen, Karl Pertsch, Oier Mees, Chelsea Finn, and Sergey Levine. Robotic control via embodied chain-of-thought reasoning. In *8th Annual Conference on Robot Learning*, 2024.
- [55] Piermarco Cannarsa, Marc-Olivier Czarnecki, et al. Minkowski content for reachable sets. *manuscripta mathematica*, 131(3):507–530, 2010.
- [56] Pertti Mattila. Rectifiability; a survey. *arXiv preprint arXiv:2112.00540*, 2021.

Supplementary Material for “Action Hallucination in Generative Vision-Language-Action Models”

A Topological Barrier: Proofs and Additional Details

A.1 Proof of Topological Barrier (Lemma 9)

Lemma 9 (Topological Barrier). *Suppose Assumption 8 holds and there exist $z_L, z_R \in \mathcal{Z}$ such that $\pi_\theta(s, z_L) \in U_L$ and $\pi_\theta(s, z_R) \in U_R$. Define the seam set, $\mathcal{Z}_{\text{seam}}(s) := \{z \in \mathcal{Z} : \pi_\theta(s, z) \in \mathcal{A}_{\text{forb}}(s)\}$. Then $\mathcal{Z}_{\text{seam}}(s)$ is nonempty and open in \mathcal{Z} . The hallucination probability at s is strictly positive, $H_\theta(s) = \Pr_{z \sim \rho_Z} [z \in \mathcal{Z}_{\text{seam}}(s)] > 0$.*

Proof. We fix a state s and suppress the dependence on s to avoid clutter.

Nonemptiness. By Assumption 3, \mathcal{Z} is path-connected, so there exists a continuous path $\gamma : [0, 1] \rightarrow \mathcal{Z}$ with $\gamma(0) = z_L$ and $\gamma(1) = z_R$. Define the action-space path $g : [0, 1] \rightarrow \mathcal{A}$ by $g(t) := \pi_\theta(s, \gamma(t))$. By continuity of $z \mapsto \pi_\theta(s, z)$, the map g is continuous.

By assumption, $g(0) \in U_L \subseteq \mathcal{A}_{\text{safe}}(s)$ and $g(1) \in U_R \subseteq \mathcal{A}_{\text{safe}}(s)$. If $g(t) \in \mathcal{A}_{\text{safe}}(s)$ for all $t \in [0, 1]$, then g would be a continuous path in $\mathcal{A}_{\text{safe}}(s)$ connecting a point in U_L to a point in U_R , contradicting that U_L and U_R are distinct path-connected components of $\mathcal{A}_{\text{safe}}(s)$ (Assumption 8(i)). Therefore, there exists $t^* \in (0, 1)$ such that $g(t^*) \notin \mathcal{A}_{\text{safe}}(s)$, i.e., $g(t^*) \in \mathcal{A}_{\text{forb}}(s)$. Let $z^* := \gamma(t^*)$; then $z^* \in \mathcal{Z}_{\text{seam}}(s)$, so $\mathcal{Z}_{\text{seam}}(s)$ is nonempty.

Openness. By Assumption 8(ii), $\mathcal{A}_{\text{forb}}(s)$ is open in \mathcal{A} , and by construction $\mathcal{Z}_{\text{seam}}(s) = \pi_\theta(s, \cdot)^{-1}(\mathcal{A}_{\text{forb}}(s))$. Since preimages of open sets under continuous maps are open, $\mathcal{Z}_{\text{seam}}(s)$ is open in \mathcal{Z} .

Positive probability. Pick $z^* \in \mathcal{Z}_{\text{seam}}(s)$. Since $\mathcal{Z}_{\text{seam}}(s)$ is open in \mathcal{Z} and \mathcal{Z} is open in \mathbb{R}^m , there exists $r > 0$ such that the closed ball $K := \overline{B}(z^*, r) \subset \mathcal{Z}_{\text{seam}}(s)$ and $K \subset \mathcal{Z}$. By Assumption 3, there exists $\rho_{\min}(K) > 0$ such that $\rho_Z(z) \geq \rho_{\min}(K)$ for almost every $z \in K$. Hence

$$H_\theta(s) = \Pr[Z \in \mathcal{Z}_{\text{seam}}(s)] \geq \Pr[Z \in K] = \int_K \rho_Z(z) dz \geq \rho_{\min}(K) \text{Vol}(K) > 0.$$

□

A.2 Proof of Isoperimetric Lower-Bound (Theorem 11)

Our quantitative bound follows the same isoperimetric / latent pre-image boundary methodology used to prove precision limitations for Lipschitz pushforward generative models [28, 30, 31], but we adapt this methodology to state-conditional action generation and interpret boundary mass as unsafe-action probability under a physically meaningful forbidden buffer assumption, with a local-Lipschitz typical-set correction.

Theorem 11 (Isoperimetric lower bound on action hallucination). *Fix a state s satisfying Assumption 10. Let $Z \sim \mathcal{N}(0, I_m)$ and fix a radius $R > 0$. Assume that the latent-to-action head $z \mapsto \pi_\theta(s, z)$ is L -Lipschitz on the typical-latent ball $B_R := \{z \in \mathbb{R}^m : \|z\| \leq R\}$, i.e., $\|\pi_\theta(s, z) - \pi_\theta(s, z')\| \leq L \|z - z'\| \forall z, z' \in B_R$ and $L > 0$. Let $\epsilon := W/L$. For each safe mode U_i , define the latent preimage $V_i := \pi_\theta(s, \cdot)^{-1}(U_i)$ and the in-ball mass $p_i^{(R)} := \Pr [Z \in V_i \cap B_R]$. Let $q(R) = \Pr [\|Z\| > R]$. Then the hallucination probability at s satisfies*

$$H_\theta(s) \geq \sum_{i=1}^M \left[\Phi \left(\Phi^{-1}(p_i^{(R)}) + \epsilon \right) - p_i^{(R)} \right] - q(R), \quad (1)$$

where Φ is the CDF of the standard normal distribution.

Proof. Fix s and ℓ . Let $B_R := \{z \in \mathbb{R}^m : \|z\| \leq R\}$, $Z \sim \mathcal{N}(0, I_m)$, and let $\gamma_m(\cdot)$ denote standard Gaussian measure on \mathbb{R}^m , so that $\Pr[Z \in E] = \gamma_m(E)$ for measurable E .

For each mode U_i , define $A_i := V_i \cap B_R$, and $p_i^{(R)} := \gamma_m(A_i)$. Since U_i is closed and $z \mapsto \pi_\theta(s, z)$ is continuous, V_i is closed. Hence A_i is closed, and in particular Borel, so $p_i^{(R)}$ is well-defined and Gaussian isoperimetry applies to A_i .

Step 1: Separation of in-ball preimages. Fix $i \neq j$. If either A_i or A_j is empty, the claimed separation is trivial. Otherwise, take any $z \in A_i$ and $z' \in A_j$. Then $z, z' \in B_R$, so Lipschitzness gives $\|\pi_\theta(s, z) - \pi_\theta(s, z')\| \leq L\|z - z'\|$. Moreover, $\pi_\theta(s, z) \in U_i$ and $\pi_\theta(s, z') \in U_j$. By Assumption 10, $\text{dist}(U_i, U_j) \geq 2W$, and therefore

$$2W \leq \|\pi_\theta(s, z) - \pi_\theta(s, z')\| \leq L\|z - z'\|.$$

Thus $\|z - z'\| \geq 2W/L = 2\epsilon$. Taking the infimum over $z \in A_i$ and $z' \in A_j$ yields $\text{dist}(A_i, A_j) \geq 2\epsilon$.

Step 2: Disjoint halos and inclusion in the seam inside B_R . Fix any radius $r \in (0, \epsilon)$. For each i , define the open r -halo around A_i by $S_i^r := \{z \in \mathbb{R}^m : 0 < \text{dist}(z, A_i) < r\}$. If $A_i = \emptyset$, we take $S_i^r = \emptyset$.

Disjointness. Suppose, for contradiction, that $z \in S_i^r \cap S_j^r$ for some $i \neq j$. Then there exist $v_i \in A_i$ and $v_j \in A_j$ such that $\|z - v_i\| < r$ and $\|z - v_j\| < r$. Hence

$$\|v_i - v_j\| \leq \|v_i - z\| + \|z - v_j\| < 2r < 2\epsilon,$$

contradicting $\text{dist}(A_i, A_j) \geq 2\epsilon$. Therefore the sets $\{S_i^r\}_{i=1}^M$ are pairwise disjoint.

Halo points inside B_R map to forbidden actions. Take any $z \in S_i^r \cap B_R$. By definition of S_i^r , there exists $v \in A_i$ such that $\|z - v\| < r < \epsilon$. Since $z, v \in B_R$, Lipschitzness gives

$$\|\pi_\theta(s, z) - \pi_\theta(s, v)\| \leq L\|z - v\| < L\epsilon = W.$$

Because $v \in A_i \subseteq V_i$, we have $\pi_\theta(s, v) \in U_i$. Therefore $\text{dist}(\pi_\theta(s, z), U_i) < W$. Also, $z \in S_i^r$ implies $z \notin A_i$. Since $z \in B_R$ and $A_i = V_i \cap B_R$, it follows that $z \notin V_i$, and hence $\pi_\theta(s, z) \notin U_i$. Thus $\pi_\theta(s, z) \in \mathcal{A} \setminus U_i$ and $\text{dist}(\pi_\theta(s, z), U_i) < W$. By the forbidden-buffer condition in Assumption 10, $\pi_\theta(s, z) \in \mathcal{A}_{\text{forb}}(s)$. Therefore $z \in \mathcal{Z}_{\text{seam}}(s)$, and we conclude

$$\bigcup_{i=1}^M (S_i^r \cap B_R) \subseteq \mathcal{Z}_{\text{seam}}(s).$$

Step 3: Gaussian isoperimetry. For $r \in (0, \epsilon)$, let $A_i^r := \{z \in \mathbb{R}^m : \text{dist}(z, A_i) < r\}$ denote the open r -neighborhood of A_i . Since A_i is closed, $S_i^r = A_i^r \setminus A_i$. Hence

$$\Pr[Z \in S_i^r] = \gamma_m(A_i^r) - \gamma_m(A_i) = \gamma_m(A_i^r) - p_i^{(R)}.$$

By the Gaussian isoperimetric inequality,

$$\gamma_m(A_i^r) \geq \Phi\left(\Phi^{-1}(p_i^{(R)}) + r\right).$$

Therefore

$$\Pr[Z \in S_i^r] \geq \Phi\left(\Phi^{-1}(p_i^{(R)}) + r\right) - p_i^{(R)}.$$

Step 4: Sum halos and apply the tail correction. Since the halos S_i^r are pairwise disjoint,

$$\Pr\left[Z \in \bigcup_{i=1}^M S_i^r\right] = \sum_{i=1}^M \Pr[Z \in S_i^r].$$

Moreover,

$$\begin{aligned} \Pr\left[Z \in \bigcup_{i=1}^M (S_i^r \cap B_R)\right] &= \Pr\left[Z \in \bigcup_{i=1}^M S_i^r\right] - \Pr\left[Z \in \left(\bigcup_{i=1}^M S_i^r\right) \cap B_R^c\right] \\ &\geq \Pr\left[Z \in \bigcup_{i=1}^M S_i^r\right] - \Pr[Z \in B_R^c]. \end{aligned}$$

Combining this with Step 2 gives

$$\begin{aligned} H_\theta(s) &= \Pr[Z \in \mathcal{Z}_{\text{seam}}(s)] \\ &\geq \Pr\left[Z \in \bigcup_{i=1}^M (S_i^r \cap B_R)\right] \\ &\geq \sum_{i=1}^M \Pr[Z \in S_i^r] - \Pr[\|Z\| > R] \\ &\geq \sum_{i=1}^M \left[\Phi\left(\Phi^{-1}(p_i^{(R)}) + r\right) - p_i^{(R)}\right] - q(R). \end{aligned}$$

This bound holds for every $r \in (0, \epsilon)$. Letting $r \uparrow \epsilon$ and using continuity of Φ , we obtain

$$H_\theta(s) \geq \sum_{i=1}^M \left[\Phi\left(\Phi^{-1}(p_i^{(R)}) + \epsilon\right) - p_i^{(R)} \right] - q(R).$$

□

Remark: Small ϵ regime. In the situation where ϵ is small, we can obtain that

$$H_\theta(s) \geq \epsilon \sum_{i=1}^M \phi(\Phi^{-1}(p_i^{(R)})) - q(R) - O(\epsilon^2), \quad (4)$$

where ϕ is the standard normal PDF. To see this, fix i and write $x_i := \Phi^{-1}(p_i^{(R)})$, so that $\Phi(x_i) = p_i^{(R)}$. Taylor's theorem with Lagrange remainder gives

$$\Phi(x_i + \epsilon) = \Phi(x_i) + \epsilon \phi(x_i) + \frac{\epsilon^2}{2} \Phi''(\xi_i)$$

for some ξ_i between x_i and $x_i + \epsilon$. Since $\Phi'(x) = \phi(x)$ and $\Phi''(x) = -x\phi(x)$, and $\sup_{x \in \mathbb{R}} |x\phi(x)| = 1/\sqrt{2\pi e}$, we obtain the uniform bound

$$\Phi(x_i + \epsilon) - p_i^{(R)} = \epsilon \phi(x_i) + O(\epsilon^2) \quad \text{with } |O(\epsilon^2)| \leq \frac{\epsilon^2}{2\sqrt{2\pi e}}.$$

Summing over i and subtracting $\Pr[\|Z\| > R]$ yields (4).

Remark: Optimizing over the typical-set radius R . We can tighten the bound in Theorem 11; for any $R > 0$ such that $\pi(s, \cdot)$ is Lipschitz on B_R with constant L_R , define $\epsilon_R = W/L_R$. Then (1) holds with ϵ replaced by ϵ_R and $H_\theta(s)$ is lower bounded by the supremum of the RHS over R ,

$$H_\theta(s) \geq \sup_{R>0: L_R < \infty} \left\{ \sum_{i=1}^M \left[\Phi\left(\Phi^{-1}(p_i^{(R)}) + \epsilon_R\right) - p_i^{(R)} \right] - q(R) \right\}$$

B Precision Barrier: Proofs and Additional Details

B.1 Proof of Precision Barrier (Lemma 13)

We will make use of the following lemma about the volume of tubular neighborhoods, which is based on Theorem A in [55].

Lemma 20 (Volume of Tubes Around Submanifolds). *Let $\mathcal{M} \subset \mathbb{R}^d$ be a compact C^1 submanifold of dimension $k < d$. Then there exist constants $C_{\mathcal{M}} > 0$ and $\bar{\delta} > 0$ such that for all $0 < \delta \leq \bar{\delta}$,*

$$\text{Vol}(\mathcal{M}_\delta) \leq C_{\mathcal{M}} \delta^{d-k},$$

where Vol denotes the d -dimensional Lebesgue measure.

Proof. For $\delta > 0$, \mathcal{M}_δ is the closed δ -neighborhood of \mathcal{M} :

$$\mathcal{M}_\delta = \overline{B}(\mathcal{M}, \delta) := \{x \in \mathbb{R}^d : \text{dist}(x, \mathcal{M}) \leq \delta\}.$$

Let

$$\omega_m := \text{Vol}_m(B_{\mathbb{R}^m}(0, 1))$$

denote the m -dimensional Lebesgue volume of the unit Euclidean ball. Since \mathcal{M} is a compact C^1 k -dimensional submanifold of \mathbb{R}^d , it is k -rectifiable [56]. Hence Theorem A [55] applies with $n = d$ and $p = k$, and yields the existence of the (finite) limit

$$\lim_{\delta \rightarrow 0^+} \frac{\text{Vol}(\mathcal{M}_\delta)}{\omega_{d-k} \delta^{d-k}} =: \text{Area}_k(\mathcal{M}),$$

where $\text{Area}_k(\mathcal{M})$ denotes the intrinsic k -dimensional surface area of \mathcal{M} (i.e., the k -dimensional Hausdorff measure). Let $L_{\mathcal{M}} := \text{Area}_k(\mathcal{M})$ and define

$$f(\delta) := \frac{\text{Vol}(\mathcal{M}_\delta)}{\omega_{d-k} \delta^{d-k}}.$$

Then $\lim_{\delta \rightarrow 0^+} f(\delta) = L_{\mathcal{M}}$. Taking $\varepsilon = 1$ in the definition of convergence, there exists $\delta_0 > 0$ such that for all $0 < \delta < \delta_0$,

$$|f(\delta) - L_{\mathcal{M}}| < 1 \quad \Rightarrow \quad f(\delta) < L_{\mathcal{M}} + 1.$$

Set $\bar{\delta} := \delta_0/2$. Then for all $0 < \delta \leq \bar{\delta}$, $f(\delta) \leq L_{\mathcal{M}} + 1$. Multiplying through gives

$$\text{Vol}(\mathcal{M}_\delta) \leq \underbrace{\omega_{d-k}(L_{\mathcal{M}} + 1)}_{C_{\mathcal{M}}} \delta^{d-k}$$

□

Using Lemma 20, we prove our precision barrier below.

Lemma 13 (Precision Barrier). *Fix a state s and adopt Definition 12. Assume that the induced action law $\mu_\theta(\cdot | s)$ is absolutely continuous with respect to d -dimensional Lebesgue measure on \mathcal{A} , with density $p(\cdot | s)$. Then, there exist constants $C_{\mathcal{M}} > 0$ and $\bar{\delta} > 0$ (depending only on \mathcal{M}) such that for all $0 < \delta \leq \bar{\delta}$, $S_\theta(s; \delta) \leq C_{\mathcal{M}} \delta^{d-k} \cdot \text{ess sup}_{a \in \mathcal{M}_\delta} p(a | s)$, and hence*

$$H_\theta(s; \delta) \geq 1 - C_{\mathcal{M}} \delta^{d-k} \cdot \text{ess sup}_{a \in \mathcal{M}_\delta} p(a | s). \quad (2)$$

Proof. Fix $0 < \delta \leq \bar{\delta}$ (where $\bar{\delta}$ will be chosen below). Since $\mathcal{A}_{\text{safe}}(s; \delta) \subseteq \mathcal{M}_\delta$ and $p(\cdot | s) \geq 0$,

$$S_\theta(s; \delta) = \int_{\mathcal{A}_{\text{safe}}(s; \delta)} p(a | s) da \leq \int_{\mathcal{M}_\delta} p(a | s) da.$$

Since $p(a | s) \leq \text{ess sup}_{u \in \mathcal{M}_\delta} p(u | s)$ for almost every $a \in \mathcal{M}_\delta$,

$$\int_{\mathcal{M}_\delta} p(a | s) da \leq \text{Vol}(\mathcal{M}_\delta) \cdot \text{ess sup}_{a \in \mathcal{M}_\delta} p(a | s).$$

Applying Lemma 20 to the compact C^1 k -submanifold $\mathcal{M} \subset \mathbb{R}^d$ provides constants $C_{\mathcal{M}} > 0$ and $\bar{\delta} > 0$ such that for all $0 < \delta \leq \bar{\delta}$,

$$\text{Vol}(\mathcal{M}_\delta) \leq C_{\mathcal{M}} \delta^{d-k}.$$

Combining the above yields

$$S_\theta(s; \delta) \leq C_{\mathcal{M}} \delta^{d-k} \cdot \text{ess sup}_{a \in \mathcal{M}_\delta} p(a | s),$$

and therefore

$$H_\theta(s; \delta) = 1 - S_\theta(s; \delta) \geq 1 - C_{\mathcal{M}} \delta^{d-k} \cdot \text{ess sup}_{a \in \mathcal{M}_\delta} p(a | s).$$

Note that if $H_\theta(s; \delta) \leq \eta$, then $S_\theta(s; \delta) \geq 1 - \eta$, and rearranging the success bound gives

$$\text{ess sup}_{a \in \mathcal{M}_\delta} p(a | s) \geq \frac{1 - \eta}{C_{\mathcal{M}}} \delta^{-(d-k)}.$$

□

B.2 Proof of Generative Trilemma (Theorem 14)

Theorem 14 (The Precision Trilemma: Collapse, Fold, or Hallucinate). *Let $m = d$ and let the action be generated by $a = F(z)$ where $Z \sim p_Z$. Assume F is C^1 on an open set $U \subseteq \mathcal{Z}$ containing the support of p_Z , with bounded latent density $\rho_Z(z) \leq \rho_Z^{\max}$. Define the active latent set as $Z_\delta := F^{-1}(\mathcal{M}_\delta) \cap U$. Define local folding and local conditioning restricted to this active set: $N_\delta := \text{ess sup}_{a \in \mathcal{M}_\delta} \#\{z \in Z_\delta : F(z) = a\}$, and $\sigma_*(\delta) := \text{ess inf}_{z \in Z_\delta} \sigma_{\min}(J_F(z))$, where $J_F(z)$ is the Jacobian of F and $\sigma_{\min}(J_F(z))$ its smallest singular value. Assume F is finite-to-one on Z_δ (i.e., $N_\delta < \infty$) and $\sigma_*(\delta) > 0$. Then the induced action distribution admits a density on \mathcal{M}_δ and the hallucination rate*

satisfies $H_\theta(s; \delta) \geq 1 - C_{\mathcal{M}} \delta^{d-k} N_\delta \rho_Z^{\max} \sigma_*(\delta)^{-d}$. If the policy achieves a target hallucination level $H_\theta(s; \delta) \leq \eta$ for some $\eta \in (0, 1)$, then the generator must satisfy

$$\underbrace{N_\delta}_{\text{Fold}} \cdot \underbrace{\sigma_*(\delta)^{-d}}_{\text{Collapse}} \geq \frac{1 - \eta}{C_{\mathcal{M}} \rho_Z^{\max}} \delta^{-(d-k)}. \quad (3)$$

Hence, as precision tightens ($\delta \rightarrow 0$), any policy that maintains $H_\theta(s; \delta) \leq \eta$ must either fold space ($N_\delta \rightarrow \infty$) or collapse volume locally ($\sigma_*(\delta) \rightarrow 0$).

Proof. Consider the active set $Z_\delta = F^{-1}(\mathcal{M}_\delta) \cap U$. Since $\sigma_{\min}(J_F(z)) \geq \sigma_*(\delta) > 0$ for almost every $z \in Z_\delta$, the Inverse Function Theorem implies that F is a local diffeomorphism in a neighborhood of any point in Z_δ . Since $\text{supp}(p_Z) \subseteq U$, the density of the pushforward distribution $a = F(z)$ is fully determined by preimages in U . Using the Area Formula (change-of-variables for many-to-one maps), for almost every $a \in \mathcal{M}_\delta$:

$$p(a | s) = \sum_{z \in F^{-1}(a) \cap U} \rho_Z(z) |\det J_F(z)|^{-1}.$$

If $a \in \mathcal{M}_\delta$, then any preimage $z \in F^{-1}(a) \cap U$ lies in Z_δ by definition. We bound the terms uniformly:

1. Density: $\rho_Z(z) \leq \rho_Z^{\max}$.
2. Jacobian: for $z \in Z_\delta$, $|\det J_F(z)| \geq (\sigma_{\min}(J_F(z)))^d \geq \sigma_*(\delta)^d$.

Substituting these bounds into the sum gives, for a.e. $a \in \mathcal{M}_\delta$,

$$\begin{aligned} p(a | s) &\leq \sum_{z \in F^{-1}(a) \cap U} \frac{\rho_Z^{\max}}{\sigma_*(\delta)^d} \\ &= \#\{z \in Z_\delta : F(z) = a\} \cdot \rho_Z^{\max} \cdot \sigma_*(\delta)^{-d}. \end{aligned}$$

Taking the essential supremum over $a \in \mathcal{M}_\delta$ yields

$$\text{ess sup}_{a \in \mathcal{M}_\delta} p(a | s) \leq N_\delta \rho_Z^{\max} \sigma_*(\delta)^{-d}.$$

Applying Lemma 13,

$$H_\theta(s; \delta) \geq 1 - C_{\mathcal{M}} \delta^{d-k} \cdot \text{ess sup}_{a \in \mathcal{M}_\delta} p(a | s).$$

Finally, if $H_\theta(s; \delta) \leq \eta$, then the lower bound must not exceed η , i.e.,

$$1 - C_{\mathcal{M}} \delta^{d-k} N_\delta \rho_Z^{\max} \sigma_*(\delta)^{-d} \leq \eta,$$

which we can rearrange to (3). \square

B.3 Proof of K-step tradeoff (Corollary 15)

Corollary 15 (*K-step precision tradeoff*). Assume the decoder is a K -step composition $F^{(K)} = \Phi_{K-1} \circ \dots \circ \Phi_0$, where each Φ_t is a C^1 diffeomorphism and there exist constants $\lambda_t > 0$ such that $\sigma_{\min}(J\Phi_t(z)) \geq \lambda_t$ for all z . Let $\sigma_*(\delta) \geq \inf_{z \in Z_\delta} \sigma_{\min}(JF^{(K)}(z)) \geq \prod_{t=0}^{K-1} \lambda_t$. Then, for all $0 < \delta \leq \bar{\delta}$, $H_\theta^{(K)}(s; \delta) \geq 1 - C_{\mathcal{M}} \rho_Z^{\max} \left(\prod_{t=0}^{K-1} \lambda_t \right)^{-d} \delta^{d-k}$. In particular, if $\lambda_t \geq \lambda \in (0, 1)$ for all t , then a necessary condition to bound the hallucination rate $H_\theta^{(K)}(s; \delta) \leq \eta \in (0, 1)$ is $K \geq \frac{1}{d \log(1/\lambda)} \left[(d-k) \log \frac{1}{\delta} + \log \frac{1-\eta}{C_{\mathcal{M}} \rho_Z^{\max}} \right]$.

Proof. Since each Φ_t is a diffeomorphism, their composition $F^{(K)}$ is a diffeomorphism, hence $N_\delta = 1$. The singular-value lower bound follows from the chain rule and the standard inequality $\sigma_{\min}(AB) \geq \sigma_{\min}(A)\sigma_{\min}(B)$. Apply Theorem 14 with $N_\delta = 1$ and $\sigma_*(\delta) \geq \prod_t \lambda_t$ to obtain the hallucination bound. Rearranging and taking logs gives the number of required steps K . Note that the bound is vacuous when the right-hand side is negative. \square

C Planning Hallucinations: Proofs and Additional Details

C.1 Proof for Horizon Barrier (Lemma 16)

Lemma 16 (Horizon Barrier). *Let $(S_t)_{t=0}^T$ be the rollout from s_0 . Define $p_t(s) := \Pr_{Z \sim p_Z} [\pi_\theta(s, Z) \in \mathcal{A}_{\text{prog}}(s, t)]$ and $\gamma_t := \sup_{s \in \Sigma_t} p_t(s)$. Then the rollout success probability factorizes and is upper bounded by $\Pr[f_{\text{plan}}(s_0, \tau_\theta(s_0, Z_{0:T-1})) = 1] \leq \prod_{t=1}^T \gamma_t$. Hence, $H_{\pi_\theta}^{\text{plan}}(I) \geq 1 - \prod_{t=1}^T \gamma_t$. In particular, if $\gamma_t \leq \gamma < 1$ for all t , then $\Pr[f_{\text{plan}}(s_0, \tau_\theta) = 1] \leq \gamma^T$ and $H_{\pi_\theta}^{\text{plan}}(I) \geq 1 - \gamma^T$.*

Proof. Let $E_k := \{\pi_\theta(S_k, Z_k) \in \mathcal{A}_{\text{prog}}(S_k, T - k)\}$ for $k = 0, \dots, T - 1$. Under deterministic dynamics and the definition of $\mathcal{A}_{\text{prog}}$, the plan is valid if and only if $\bigcap_{k=0}^{T-1} E_k$ occurs. By the chain rule,

$$\Pr \left[\bigcap_{k=0}^{T-1} E_k \right] = \prod_{k=0}^{T-1} \Pr[E_k \mid E_0 \cap \dots \cap E_{k-1}] = \prod_{t=1}^T \eta_t,$$

where we re-indexed with $t = T - k$, i.e., $\eta_t := \Pr[E_{T-t} \mid E_0 \cap \dots \cap E_{T-t-1}]$

On the event $E_0 \cap \dots \cap E_{T-t-1}$, the rollout state S_{T-t} must lie in Σ_t by definition of $\mathcal{A}_{\text{prog}}(S_{T-t-1}, t + 1)$ and Σ_t . Therefore $p_t(S_{T-t}) \leq \sup_{s \in \Sigma_t} p_t(s) = \gamma_t$ pointwise on this event, implying $\eta_t \leq \gamma_t$. Hence

$$\Pr[f_{\text{plan}} = 1] = \prod_{t=1}^T \eta_t \leq \prod_{t=1}^T \gamma_t,$$

and the hallucination bounds follow by complement. The γ^T specialization is immediate when $\gamma_t \leq \gamma$ for all t . \square

C.2 Proof for Reliability search budget window

Lemma 18 (Reliability search-budget window). *Consider any verification-guided planner with budget q , verifier error rates $(\varepsilon_{\text{fp}}, \varepsilon_{\text{fn}})$, and amplification schedule $(\rho_j)_{j=1}^q$. Let $c := 1 - \varepsilon_{\text{fn}}$. Then $H(I) \leq \varepsilon_{\text{fp}} \sum_{j=1}^q \Pr[C_{j-1}](1 - \rho_j) \leq q\varepsilon_{\text{fp}}$ and $A(I) \leq \prod_{j=1}^q (1 - c\rho_j)$. Consequently, the planner is certified as (α, β) -reliable whenever $\varepsilon_{\text{fp}} \sum_{j=1}^q \Pr[C_{j-1}](1 - \rho_j) \leq \alpha$ and $\prod_{j=1}^q (1 - c\rho_j) \leq \beta$. The simpler sufficient certificate $q\varepsilon_{\text{fp}} \leq \alpha$ and $\prod_{j=1}^q (1 - c\rho_j) \leq \beta$ also certifies (α, β) -reliability.*

Proof. Let \mathcal{F}_{j-1} denote the σ -field generated by the planner's history up to round $j - 1$, including past proposals and verifier outcomes. On C_{j-1} , the proposal distribution Q_j is \mathcal{F}_{j-1} -measurable and $\tau_j \sim Q_j$.

Hallucination bound. Let

$$F_j := \{C_{j-1} \wedge \tau_j \notin V \wedge \tilde{f}_j(\tau_j) = 1\}$$

be the event that round j produces a false acceptance. If the planner outputs an invalid candidate, then exactly one of the events F_1, \dots, F_q occurs. Thus

$$H(I) = \sum_{j=1}^q \Pr[F_j].$$

By the conditional false-positive guarantee, for every history and proposed invalid candidate $\tau \in V^c$,

$$\Pr[\tilde{f}_j(\tau) = 1 \mid \mathcal{F}_{j-1}, \tau_j = \tau] \leq \varepsilon_{\text{fp}}.$$

Therefore, conditioning on \mathcal{F}_{j-1} ,

$$\begin{aligned} \Pr[F_j \mid \mathcal{F}_{j-1}] &= \mathbf{1}\{C_{j-1}\} \int_{V^c} Q_j(d\tau) \Pr[\tilde{f}_j(\tau) = 1 \mid \mathcal{F}_{j-1}, \tau_j = \tau] \\ &\leq \mathbf{1}\{C_{j-1}\} \varepsilon_{\text{fp}} Q_j(V^c) \\ &= \mathbf{1}\{C_{j-1}\} \varepsilon_{\text{fp}} (1 - Q_j(V)). \end{aligned}$$

Taking expectations gives

$$\Pr[F_j] \leq \varepsilon_{\text{fp}} \mathbb{E}[\mathbf{1}\{C_{j-1}\}(1 - Q_j(V))].$$

By the definition of ρ_j , with the stated convention when $\Pr[C_{j-1}] = 0$,

$$\mathbb{E}[\mathbf{1}\{C_{j-1}\}(1 - Q_j(V))] = \Pr[C_{j-1}](1 - \rho_j).$$

Hence

$$H(I) \leq \varepsilon_{\text{fp}} \sum_{j=1}^q \Pr[C_{j-1}](1 - \rho_j) \leq q\varepsilon_{\text{fp}}.$$

Abstention bound. Let C_j be the event that the planner reaches round $j + 1$, equivalently that no acceptance occurred in rounds $1, \dots, j$. Then $A(I) = \Pr[C_q]$ and C_0 is the sure event. Let T_j be the event that round j gives a true acceptance:

$$T_j := \{C_{j-1} \wedge \tau_j \in V \wedge \tilde{f}_j(\tau_j) = 1\}.$$

Using the conditional true-acceptance guarantee,

$$\begin{aligned} \Pr[T_j] &\geq c \mathbb{E}[\mathbf{1}\{C_{j-1}\}Q_j(V)] \\ &= c \Pr[C_{j-1}]\rho_j. \end{aligned}$$

Since every true acceptance prevents reaching the next round,

$$\begin{aligned} \Pr[C_j] &\leq \Pr[C_{j-1}] - \Pr[T_j] \\ &\leq \Pr[C_{j-1}](1 - c\rho_j). \end{aligned}$$

This recursive inequality remains valid when $\Pr[C_{j-1}] = 0$. Iterating from $\Pr[C_0] = 1$ yields

$$A(I) = \Pr[C_q] \leq \prod_{j=1}^q (1 - c\rho_j).$$

The certification statements follow by requiring the corresponding upper bounds on $H(I)$ and $A(I)$ to be at most α and β , respectively. \square

C.3 Non-adaptive proposal-and-verify window and horizon fragility

Lemma 18 is a useful tool to study how fast adaptation must take place. We first specialize it to the common non-adaptive case, where the planner repeatedly samples from the same proposal distribution and only uses the verifier as an accept/reject filter.

Corollary 21 (Non-adaptive proposal-and-verify window and horizon fragility). *Consider the verification-guided planner of Lemma 18. Assume it is non-adaptive in the sense that, on every reached round, $Q_j = Q$ for a fixed proposal distribution Q over \mathcal{P}_I . Let $\rho := Q(V)$ and $c := 1 - \varepsilon_{\text{fn}}$. Then*

$$H(I) \leq \varepsilon_{\text{fp}}(1 - \rho) \sum_{j=1}^q \Pr[C_{j-1}] \leq q\varepsilon_{\text{fp}}(1 - \rho) \leq q\varepsilon_{\text{fp}},$$

and

$$A(I) \leq (1 - c\rho)^q.$$

Consequently, if $\beta \in (0, 1)$, $c\rho \in (0, 1)$, and $\varepsilon_{\text{fp}}(1 - \rho) > 0$, the sharper non-adaptive certification window is

$$\frac{\log \beta}{\log(1 - c\rho)} \leq q \leq \frac{\alpha}{\varepsilon_{\text{fp}}(1 - \rho)}.$$

The cruder instance-independent upper bound $q \leq \alpha/\varepsilon_{\text{fp}}$ also suffices when $\varepsilon_{\text{fp}} > 0$. If $\varepsilon_{\text{fp}}(1 - \rho) = 0$, the non-adaptive false-positive certificate imposes no upper bound on q .

Moreover, assume $c > 0$, $\beta \in (0, 1)$, and $\rho > 0$. If Q is induced by rolling out a T -step sequential policy and the horizon barrier gives $\rho = Q(V) \leq \gamma^T$ for some $\gamma \in (0, 1)$, then any q satisfying the abstention certificate $(1 - c\rho)^q \leq \beta$ obeys

$$q \geq \frac{\log(1/\beta)}{-\log(1 - c\rho)} \geq \frac{\log(1/\beta)}{-\log(1 - c\gamma^T)}.$$

In particular, when $c\gamma^T \leq 1/2$, this certificate requires

$$q \geq \frac{1}{2c} \gamma^{-T} \log(1/\beta),$$

which is exponential in T .

Proof. In the non-adaptive case, $Q_j = Q$ on every reached round. For false acceptances, the proof of Lemma 18 gives directly

$$\Pr[F_j] \leq \varepsilon_{\text{fp}} \mathbb{E}[\mathbf{1}\{C_{j-1}\}(1 - Q(V))] = \varepsilon_{\text{fp}}(1 - \rho) \Pr[C_{j-1}],$$

and summing over j yields the stated hallucination bound. Similarly, at each reached round the true-acceptance probability is at least $c\rho$, so

$$\Pr[C_j] \leq \Pr[C_{j-1}](1 - c\rho).$$

Iterating gives $A(I) \leq (1 - c\rho)^q$.

The certification window follows by enforcing $q\varepsilon_{\text{fp}}(1 - \rho) \leq \alpha$ and $(1 - c\rho)^q \leq \beta$. Since $\beta \in (0, 1)$ and $c\rho \in (0, 1)$, taking logs in the abstention inequality gives $q \geq \log \beta / \log(1 - c\rho)$.

For the horizon-fragility statement, the abstention certificate implies

$$q \geq \frac{\log(1/\beta)}{-\log(1 - c\rho)}.$$

The map $x \mapsto -\log(1 - cx)$ is increasing on $[0, 1/c]$ for $c > 0$. Since $\rho \leq \gamma^T$, the denominator is at most $-\log(1 - c\gamma^T)$, giving

$$q \geq \frac{\log(1/\beta)}{-\log(1 - c\gamma^T)}.$$

Finally, if $x := c\gamma^T \leq 1/2$, then $-\log(1 - x) \leq 2x$, and therefore

$$q \geq \frac{1}{2c} \gamma^{-T} \log(1/\beta).$$

□

C.4 Cumulative valid-mass condition for abstention control

Corollary 22 (Cumulative valid-mass condition for abstention control). *Under the assumptions of Lemma 18,*

$$A(I) \leq \exp\left(-c \sum_{j=1}^q \rho_j\right).$$

If $c > 0$ and $\beta \in (0, 1)$, a sufficient condition for $A(I) \leq \beta$ is

$$\sum_{j=1}^q \rho_j \geq c^{-1} \log(1/\beta).$$

Proof. From Lemma 18,

$$A(I) \leq \prod_{j=1}^q (1 - c\rho_j).$$

Since $c\rho_j \geq 0$ and $1 - x \leq e^{-x}$ for all $x \geq 0$,

$$\prod_{j=1}^q (1 - c\rho_j) \leq \prod_{j=1}^q e^{-c\rho_j} = \exp\left(-c \sum_{j=1}^q \rho_j\right).$$

The sufficient condition follows by rearranging $\exp(-c \sum_j \rho_j) \leq \beta$. □

C.5 Proof for Amplification-rate to beat the horizon barrier

Theorem 19 (Amplification-rate to beat the horizon barrier). *Consider the planner above, with amplification schedule $(\rho_j)_{j=1}^q$. Any (α, β) -reliable planner must satisfy $\sum_{j=1}^q \Pr[C_{j-1}]\rho_j \geq 1 - \alpha - \beta$. Assume an exponentially small initial valid mass $\rho_1 \leq \gamma^T$ for some $\gamma \in (0, 1)$. Then (i) **Polynomial amplification is insufficient**. If $\rho_j \leq \rho_1 j^p$ for some fixed $p \geq 0$, then meeting the necessary condition requires $q \geq \left(1 + \frac{(p+1)(1-\alpha-\beta)}{\gamma^T}\right)^{1/(p+1)} - 1$. For fixed $p, \gamma \in (0, 1)$, and nontrivial reliability target $1 - \alpha - \beta > 0$, this lower bound grows exponentially in T ; (ii)*

Geometric amplification is sufficient, if within the verifier budget. Assume $c := 1 - \varepsilon_{\text{fn}} > 0$, $\beta \in (0, 1)$, and $\rho_j \geq \min\{1, \rho_1 r^{j-1}\}$ for some $r > 1$. Then $q\varepsilon_{\text{fp}} \leq \alpha$ and $\sum_{j=1}^q \min\{1, \rho_1 r^{j-1}\} \geq c^{-1} \log(1/\beta)$ certify (α, β) -reliability. In the unsaturated regime $\rho_1 r^{q-1} \leq 1$, the second condition becomes $\rho_1 \frac{r^q - 1}{r - 1} \geq c^{-1} \log(1/\beta)$ and it suffices that $q \geq \log_r \left(1 + \frac{(r-1)c^{-1} \log(1/\beta)}{\rho_1} \right)$. Thus, for fixed $r > 1$, $c > 0$, and $\beta \in (0, 1)$, the geometric cumulative-mass condition is achieved at $q = \Theta(\log 1/\rho_1)$ rounds. If $\rho_1 \asymp \gamma^T$, this becomes $q = \Theta(T)$.

Proof. Define the valid set of plans,

$$E_{\text{val}} := \{\hat{\tau} \neq \perp \wedge \hat{\tau} \in V\},$$

so $S(I) = \Pr[E_{\text{val}}]$. If the planner outputs a valid candidate, then some reached round must have proposed a valid candidate. Therefore

$$E_{\text{val}} \subseteq \bigcup_{j=1}^q (C_{j-1} \cap \{\tau_j \in V\}).$$

By the union bound,

$$\begin{aligned} S(I) &\leq \sum_{j=1}^q \Pr[C_{j-1} \cap \{\tau_j \in V\}] \\ &= \sum_{j=1}^q \Pr[C_{j-1}] \rho_j \leq \sum_{j=1}^q \rho_j. \end{aligned}$$

If the planner is (α, β) -reliable, then $S(I) = 1 - A(I) - H(I) \geq 1 - \alpha - \beta$. Hence

$$\sum_{j=1}^q \Pr[C_{j-1}] \rho_j \geq 1 - \alpha - \beta, \quad \sum_{j=1}^q \rho_j \geq 1 - \alpha - \beta.$$

(i) If $\rho_j \leq \rho_1 j^p$ and $\rho_1 \leq \gamma^T$, then

$$\sum_{j=1}^q \rho_j \leq \gamma^T \sum_{j=1}^q j^p \leq \gamma^T \frac{(q+1)^{p+1} - 1}{p+1},$$

where the last inequality follows from $\sum_{j=1}^q j^p \leq \int_0^q (x+1)^p dx$. Combining this upper bound with the necessary condition and rearranging gives

$$q \geq \left(1 + \frac{(p+1)(1-\alpha-\beta)}{\gamma^T} \right)^{1/(p+1)} - 1.$$

For fixed $p, \gamma \in (0, 1)$, and $1 - \alpha - \beta > 0$, this grows exponentially in T .

(ii) Lemma 18 gives $H(I) \leq q\varepsilon_{\text{fp}}$, so $q\varepsilon_{\text{fp}} \leq \alpha$ certifies the hallucination constraint. The same lemma also gives

$$A(I) \leq \prod_{j=1}^q (1 - c\rho_j) \leq \exp \left(-c \sum_{j=1}^q \rho_j \right),$$

using $1 - x \leq e^{-x}$. Under the assumed geometric lower bound,

$$\sum_{j=1}^q \rho_j \geq \sum_{j=1}^q \min\{1, \rho_1 r^{j-1}\}.$$

Thus $A(I) \leq \beta$ is certified whenever

$$\sum_{j=1}^q \min\{1, \rho_1 r^{j-1}\} \geq c^{-1} \log(1/\beta).$$

If $\rho_1 r^{q-1} \leq 1$, this sum is $\rho_1 (r^q - 1)/(r - 1)$, giving the displayed unsaturated sufficient condition and the equivalent lower bound on q within that regime.

It remains to justify the stated $\Theta(\log(1/\rho_1))$ scaling for the geometric cumulative-mass condition. Let $L := c^{-1} \log(1/\beta) > 0$ be fixed. For an upper bound, take

$$q = \lceil \log_r(1/\rho_1) \rceil + \lceil L \rceil + 1.$$

By this time the terms $\min\{1, \rho_1 r^{j-1}\}$ have saturated, and there are at least $\lceil L \rceil$ unit terms, so the cumulative mass is at least L . Thus $q = O(\log(1/\rho_1))$ suffices. For a lower bound, if $q \leq \frac{1}{2} \log_r(1/\rho_1)$, then all terms are unsaturated for small ρ_1 and

$$\sum_{j=1}^q \min\{1, \rho_1 r^{j-1}\} \leq \frac{\rho_1 r^q}{r-1} \leq \frac{\rho_1^{1/2}}{r-1} \rightarrow 0,$$

which is eventually smaller than the fixed positive threshold L . Hence any q satisfying the cumulative-mass condition is $\Omega(\log(1/\rho_1))$, and the scaling is $\Theta(\log(1/\rho_1))$. If $\rho_1 \asymp \gamma^T$, this becomes $\Theta(T)$. \square

C.6 Action Chunking and the Barriers

A common intuition is that if the primitive action is very low-level (e.g., small joint deltas), then the safe set $\mathcal{A}_{\text{safe}}(s) = \{a : f_{\text{phys}}(s, a) = 1\}$ is often connected in many states, seemingly avoiding the topological barrier from Section 3.1. This is frequently true at the *one-step* level, but it does *not* remove multimodality for long-horizon goal-reaching. Chunking trades *fewer decisions* against a *harder per-decision sampling problem*:

1. *Topology reappears at the progress/chunk level.* Even if $\mathcal{A}_{\text{safe}}(s)$ is connected for small one-step controls, the *progress* set $\mathcal{A}_{\text{prog}}(s, t)$ can be disconnected at reachability bottlenecks. Two small safe actions can lead into different time-bounded reachable basins Σ_{t-1} , while “in-between” actions can be safe but *non-progress* (leading to dead ends or timeouts). Chunking amplifies this effect since the progress set typically decomposes into more separated components (distinct partial trajectories/contact-mode prefixes), activating the same “seam” phenomenon from Section 3.1, now with respect to progress/plan validity rather than one-step physical invalidity.
2. *Precision compounds within a chunk.* In contact-rich tasks (Section 3.2), progress may require staying in a thin tube (or near a manifold) over multiple successive steps. Requiring consecutive steps in the chunk to remain in such a tube makes the feasible region effectively thinner, decreasing the per-sample mass of $\mathcal{A}_{\text{prog}}(s, t)$ (often sharply) as the chunk length grows.
3. *Horizon compounding improves in count, worsens in mass.* If the policy outputs chunks of length ℓ and commits to executing them, then Lemma 16 applies with an *effective* horizon of roughly $\lceil T/\ell \rceil$. Increasing ℓ reduces the number of factors in this product (helping the horizon barrier) but typically decreases each factor γ_t (harder chunk feasibility due to topology/precision and open-loop drift), creating a natural “sweet spot” in ℓ .

This view also clarifies a common empirical design; predict long chunks for temporal coherence but execute only a short prefix before replanning (receding-horizon), which reduces open-loop compounding and delays irreversible mode commitment while still leveraging temporally structured proposals.

C.7 Family-level pruning and valid-mass amplification

This appendix subsection formalizes the intuition from the VLA discussion. Fix a round j and write $\rho = Q_j(V)$. Suppose a partial check identifies a measurable family of invalid continuations $B_j \subseteq V^c$, discards this family, and preserves every valid continuation. Let Q_j^+ be the proposal distribution obtained by renormalizing Q_j on $\mathcal{P}_I \setminus B_j$. Assume $Q_j(B_j) < 1$. Then

$$Q_j^+(V) = \frac{Q_j(V)}{1 - Q_j(B_j)}.$$

If the pruning step removes at least a κ fraction of the invalid mass, namely $Q_j(B_j) \geq \kappa Q_j(V^c)$ for some $\kappa \in [0, 1]$, then

$$Q_j^+(V) \geq \frac{Q_j(V)}{1 - \kappa(1 - Q_j(V))}.$$

In particular, while $Q_j(V) \leq 1/2$,

$$Q_j^+(V) \geq \frac{Q_j(V)}{1 - \kappa/2}.$$

Thus, a pruning operation that repeatedly removes a constant fraction of the currently invalid region can multiply the valid mass by a constant factor until the distribution is no longer dominated by invalid continuations. This is a simple analysis of what hierarchical decomposition, prefix feasibility tests, early collision checks, branch-and-bound, tree search, and replanning are meant to accomplish: they eliminate families of bad futures, rather than merely rejecting isolated completed samples.

D Experimental Setup

D.1 Topology Barrier

This appendix describes the implementation and hyperparameters used for the 2D band topology experiments in which we measure action hallucination and relate it to the isoperimetric lower bound. All experiments were run on a cloud server (4 vCPUs, 15 GB Memory) with two NVIDIA T4 GPUs.

Band action-space geometry and safe modes. Actions are two-dimensional, $a = (x, y) \in \mathbb{R}^2$, with an *action band*

$$x \in [x_{\min}, x_{\max}], \quad y \in [-y_{\max}, y_{\max}].$$

Within this band, the safe set is the union of M disconnected horizontal strips $\{U_i\}_{i=1}^M$ separated by forbidden gaps. Let r denote the strip half-width and W denote the gap half-width. The strip centers are placed symmetrically about 0 with spacing $2(r + W)$, i.e.

$$\mu_i = \left(i - \frac{M-1}{2}\right) 2(r + W), \quad i \in \{0, \dots, M-1\}.$$

The safe strips are

$$U_i = \{(x, y) : x \in [x_{\min}, x_{\max}], y \in [\mu_i - r, \mu_i + r]\}.$$

Any action outside the band, or in the gaps between strips, is forbidden and counted as a hallucination.

Training data distribution. We train on i.i.d. safe actions sampled from the union of strips. In the experiments reported here, we perform the following:

- sample mode index $i \sim \text{Categorical}(\pi)$ with π uniform over modes,
- sample $x \sim \text{Uniform}[x_{\min}, x_{\max}]$,
- sample $y \sim \text{Uniform}[\mu_i - r, \mu_i + r]$.

Models. All methods produce actions deterministically from a latent/noise variable in \mathbb{R}^2 ; throughout, the base latent distribution is $Z \sim \mathcal{N}(0, I_2)$. We implemented two models:

- **Flow Matching.** We train a rectified flow vector field $v_\theta(x, t)$ with $t \in [0, 1]$ using flow-matching:

$$x_t = (1-t)x_0 + tx_1, \quad x_0 \sim p_{\text{data}}, \quad x_1 \sim \mathcal{N}(0, I_2),$$

with target velocity $v^*(x_t, t) = x_1 - x_0$, optimized via MSE $\|v_\theta(x_t, t) - v^*(x_t, t)\|_2^2$. Sampling is deterministic Euler (or Heun) integration from $t = 1$ to $t = 0$ starting at Gaussian noise.

- **Diffusion.** We train a v -pred diffusion model with cosine schedule (default $T = 200$) and exponential moving average (EMA) of parameters. Training uses MSE on the v -prediction target. Sampling is deterministic DDIM (i.e. $\eta = 0$) with a user-specified number of sampling steps.

Both the flow and diffusion networks use the same backbone: a sinusoidal time embedding of dimension 64, concatenated with the 2D input, followed by an MLP (depth 4 with hidden layers of width 256), with LayerNorm and SiLU activations, and a final linear layer to \mathbb{R}^2 . We optimize with AdamW (default learning rate 2×10^{-4} , weight decay 10^{-4}), batch size 2048, and gradient-norm clipping at 1.0. Unless otherwise stated, we train each model for 100,000 steps.

Evaluation protocol and metrics. For each configuration (defined by (M, W) and the “smoothness” settings), and for each random seed, we generate $N = 10^6$ samples in batches of 4096. For each method we compute the (i) Hallucination probability, $H = \Pr[a(Z) \notin \cup_{i=1}^M U_i]$, where any sample outside the band or in the gaps counts as forbidden, and (ii) the mode masses: $p_i = \Pr[a(Z) \in U_i]$ for $i \in \{1, \dots, M\}$. We estimate a distribution of local Lipschitz proxies on the typical latent ball $B_R = \{z : \|z\| \leq R\}$ with $R = 3.0$ by sampling 2048 points from $Z \sim \mathcal{N}(0, I_2)$ truncated to B_R , and estimating $\sigma_{\max}(z) \approx \|J(z)\|_{\text{op}}$ via finite differences with step size 0.01.

D.2 Precision Barrier

We study a controlled “glass/mug grasp” proxy in which valid actions lie on a low-dimensional manifold $\mathcal{M} \subset \mathbb{R}^d$. Similar to the topological experiments, we train two generative models (Flow Matching and Diffusion, as in the topology

experiments) on the same synthetic manifold distribution and compare them under consistent evaluation. Each action is represented by a 7D vector

$$a = [x, y, h, \text{roll}, \text{pitch}, \sin(\text{yaw}), \cos(\text{yaw})] \in \mathbb{R}^7, \quad (5)$$

where yaw is encoded as (\sin, \cos) to avoid discontinuities at $\pm\pi$. Coordinates are normalized so that a Euclidean distance meaningfully mixes translational and rotational components.

Ideal side-grasp manifold. The ideal grasp manifold \mathcal{M} is parameterized by two intrinsic coordinates:

- $\theta \in [0, 2\pi)$: angle around the mug,
- h in a valid height interval $[h_{\min}, h_{\max}]$.

This defines a $k = 2$ dimensional manifold embedded in an ambient space of dimension $d = 7$, hence codimension $d - k = 5$. Points on \mathcal{M} satisfy: (i) (x, y) lies on a ring of fixed radius r (mug radius plus clearance), (ii) roll and pitch are zero, (iii) yaw points inward toward the mug center (a deterministic function of θ), and (iv) h lies in $[h_{\min}, h_{\max}]$. For any $a \in \mathbb{R}^7$, we compute

$$\text{dist}(a, \mathcal{M}) := \|a - \Pi_{\mathcal{M}}(a)\|_2, \quad (6)$$

where $\Pi_{\mathcal{M}}$ is an analytic projection that solves for the best θ^* (by jointly aligning the (x, y) ring constraint and yaw (\sin, \cos) consistency), clamps h to $[h_{\min}, h_{\max}]$, and sets roll/pitch to 0.

Evaluation protocol and metrics. For a trained model, we generate i.i.d. samples $\{x^{(i)}\}_{i=1}^N$ and evaluate the action hallucination curve

$$H(\delta) = \mathbb{P}(\text{dist}(x, \mathcal{M}) > \delta) \approx \frac{1}{N} \sum_{i=1}^N \mathbf{1}[\text{dist}(a^{(i)}, \mathcal{M}) > \delta], \quad (7)$$

over a log-spaced grid $\delta \in [\delta_{\min}, \delta_{\max}]$. To probe whether concentration near a lower-dimensional manifold requires ill-conditioned transformations, we analyze Jacobians of sampler maps. Let a sampler consist of step maps $x_{k+1} = F_k(x_k)$, for $k = 0, \dots, K - 1$, so the overall map is $G = F_{K-1} \circ \dots \circ F_0$. We compute per-step Jacobians $J_k = \partial F_k / \partial x$ and the global Jacobian

$$J_{\text{global}} = \frac{\partial G}{\partial x} = J_{K-1} \cdots J_0. \quad (8)$$

Conditioning is summarized via singular values $\sigma_{\min}(J)$ and diagnostics are computed along random sampler trajectories initialized from Gaussian noise.

Author Contributions and LLM Usage

H. Soh conceived the central idea and wrote the majority of the manuscript. E. Lim verified the proofs and contributed improvements to the technical statements. LLMs were used to assist with idea exploration, proof development, code implementation, and manuscript editing. Illustrative images depicting the robot in various environments were generated using Gemini, while all schematic figures were created by the authors. All plots were produced from experiments described in the paper and appendix. The authors take full responsibility for the content of this work.